Accepted Manuscript

Prodrugs for nitroreductase based cancer therapy- 2 novel amide/Ntr combinations targeting PC3 cancer cells

Tuğba Güngör, Ferah Cömert Önder, Esra Tokay, Ünzile Güven Gülhan, Nelin Hacıoğlu, Tuğba Taşkın Tok, Ayhan Çelik, Feray Köçkar, Mehmet Ay

PII: S0223-5234(19)30253-3

DOI: https://doi.org/10.1016/j.ejmech.2019.03.035

Reference: EJMECH 11205

To appear in: *European Journal of Medicinal Chemistry*

Received Date: 28 December 2018

Revised Date: 26 February 2019

Accepted Date: 14 March 2019

Please cite this article as: Tuğ. Güngör, Ferah.Cö. Önder, E. Tokay, Ü.Gü. Gülhan, N. Hacıoğlu, Tuğ.Taşı. Tok, A. Çelik, F. Köçkar, M. Ay, Prodrugs for nitroreductase based cancer therapy- 2 novel amide/Ntr combinations targeting PC3 cancer cells, *European Journal of Medicinal Chemistry* (2019), doi: https://doi.org/10.1016/j.ejmech.2019.03.035.

PRODRUGS FOR NITROREDUCTASE BASED CANCER THERAPY- 2

Novel Amide/Ntr Combinations Targeting PC3 Cancer Cells

Tuğba Güngör[a], Ferah Cömert Önder[a], Esra Tokay[b], Ünzile Güven Gülhan[c], Nelin Hacıoğlu[b], Tuğba Taşkın Tok[d], Ayhan Çelik[c, #] Feray Köçkar[b], Mehmet Ay[a*]

[a]Department of Chemistry, Faculty of Sciences and Arts, Natural Products and Drug Research Laboratory, Çanakkale Onsekiz Mart University, Çanakkale 17020, Turkey

[b]Department of Molecular Biology and Genetic, Faculty of Sciences and Arts, Balıkesir University, Balıkesir 10145, Turkey

[c]Department of Chemistry, Faculty of Science, Gebze Technical University, Gebze-Kocaeli 41400, Turkey

[d]Department of Chemistry, Faculty of Sciences and Arts, Gaziantep University, Gaziantep 27310, Turkey

*Corresponding author

E-mail addresses: mehmetay06@comu.edu.tr; mehmetay06@yahoo.com (Mehmet Ay[a*]) Çanakkale Onsekiz Mart University, Faculty of Sciences and Arts, Department of Chemistry, Natural Products and Drug Research Laboratory, 17020 Çanakkale, Turkey.

[#]Ayhan Çelik was left GTU after September, 2016.

* Patent pending in preperation

ABSTRACT

The use of nitroreductases (NTR) that catalyze the reduction of nitro compounds by using NAD(P)H in GDEPT (Gene-directed enzyme prodrug therapy) studies which minimize toxicity at healthy cells and increases concentration of drugs at cancer cells is remarkable. Discovery of new prodrug/NTR combinations is necessary to be an alternative to known prodrug candidates such as CB1954, SN23862, PR-104A. For this aim, nitro containing aromatic amides **(A1-A23)** were designed, synthesized, performed in silico ADMET and molecular docking techniques in this study. Prodrug candidates were studied on reduction potentials with Ssap-NtrB by HPLC system. Also, cyototoxic properties and prodrug ability of these amides were investigated using different cancer cell lines such as Hep3B and PC3. As a result of theoretical and biological studies, combinations of **A5, A6** and **A20** with Ssap-NtrB can be suggested as potential prodrugs/enzyme combinations at NTR based cancer therapy compared with CB1954/NfsB.

Keywords: Nitro aromatic amides, Prodrug, Ssap-NtrB, Enzymatic activity, Cytotoxicity, Molecular docking.

1. INTRODUCTION

Gene-directed enzyme prodrug therapy (GDEPT) have captured the attention of the biology-medicine community since it limits toxicity at healthy cells and increases amount of drug in cancer cells for cancer therapies [1]. GDEPT mainly consists of two steps. The first step is transfer of the enzyme gene to the tumor cell by loading the carrier vector and expression of this gene in the tumor cell [2, 3]. The second step is the conversion of nontoxic prodrug to cytotoxic drug by enzyme catalysis. Finally, the active drug is transported to other cancer cells with bystander effect [4].

The use of nitroreductases (NTR) that catalyze the reduction of nitro compounds by using NAD(P)H in GDEPT studies is remarkable [2]. Reduction with NTRs can be occured in two types to form nitroso, hydroxylamine and amine metabolites [5]. Type I NTRs are oxygen insensitive and catalayze two electron reduction of the nitro group, type II NTRs are oxygen sensitive and performs single electron reduction.

5-Aziridinyl-2,4-dinitrobenzamide (CB1954), which is the prototype of the dinitrobenzamide prodrug family, has been the most successful prodrug for nitroreductases of GDEPT [2]. When CB1954 is reduced by NTR, 2-hydroxylamine and 4-hydroxylamine metabolites occur at equal amounts [6]. While 4-hydroxylamine metabolite is more cytotoxic and shows good bystander effect, 2-amino metabolite exhibits better diffusion and higher stability than the 4-hydroxylamine metabolite [7-9]. It is known that 2-hydroxylamine metabolite provides inhibitory effect on the growth of cancer cells [10, 11]. The efficacy of CB1954 in GDEPT system has been exhibited by clinical studies on prostate cancer and liver cancer [12,13]. However, due to the hepatotoxic effects of the prodrug CB1954 and low efficiency of *E. coli* NTR on CB1954, clinical trials were terminated [14,15], emphasizing the need for better prodrug alternatives and new nitroreductase enzymes [16-23]. A mustard derivative of CB1954, SN23862 (5-[*N*,*N*-bis(2-chloroethyl)amino]-2-hydroxyamino-4-nitrobenzamide) has higher K_M and k_{cat} values and better bystander effect as compared to CB1954 and is more cytotoxic when interacts with NfsB (*E.coli* nitroreductase) [24, 25]. The limitation at *in vivo* studies of first generation of dinitrobenzamide mustards (DNBM) due to their low solubility, DNBM phosphate esters have been developed as pre-prodrug. These compounds (e.g. PR-104) were firstly converted to corresponding prodrug alcohol (e.g. PR-104A) with systemic phosphate effect and the next step is reduction of prodrugs by NfsB to give active drugs (e.g. PR-104H) [26, 27] PR-104A has been found more cytotoxic in hypoxic and aerobic conditions against different cancer cells when compared to other DNBM

compounds. Preclinical studies of PR-104A has been successful and proceeded to clinical studies [28] (Figure 1). Later, it was discovered that PR-104 had a myelotoxic effect and clinical trials did not proceed further [29]. However, new studies continue to be conducted on the second generation of PR-104A analogues for the treatment of cancer [15, 19, 31].

Design and synthesis of nitro containing compounds as fluorescent imaging probes for NTR detection and diagnosis of tumor cells at hypoxic conditions have come to the fore in recent years [31-34].

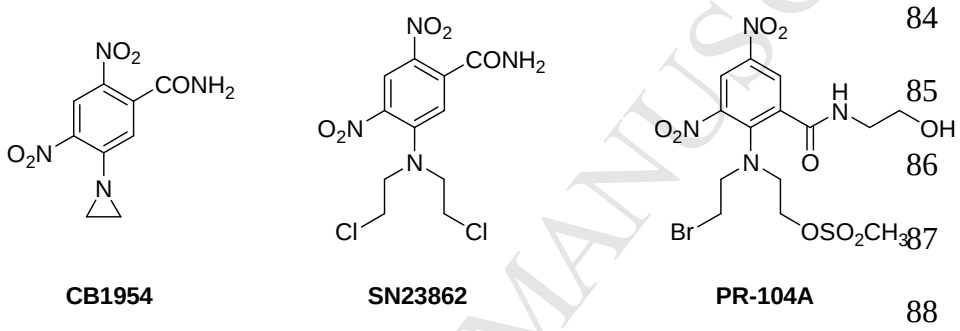

CB1954 **SN23862** **PR-104A**

Figure 1. The structures of a few reported prodrug candidates

Also it is known that benzamide derivatives have superior pharmacological properties and used as drugs (vismodegib, sonidegib, taladegib, parsalmide, tiapride etc.) in the treatment of various diseases [35-38]. In this study, nitro-containing amide prodrugs were designed on the basis of model prodrug CB1954, SN23862, PR-104A and other known benzamides.

In our previous work, we synthesized three benzamide and one hydrazide derivative as nitro bearing prodrug and investigated their enzymatic activities on Ssap-NtrB a new nitroreductase developed by our research group [18], antiproliferative effects on different cancer cells [39]. Promising results prompted us to diversify the nitro containing amides (23 compounds) and investigate more amide prodrugs to be used for Ntr-based cancer therapies. Four different amide core structures such as phenylacetamide **(A1-A4)**,

4-(4-nitrobenzoyl)morpholine/piperidine **(A5-A6)**, *N*-substitutedphenyl benzamide **(A7-A14)**, bis(4-nitrobenzamide) **(A15-A23)** were designed in this study. The main reason selecting these skeletons is to discover the most active structure among these four type compounds that more interacting with the Ssap-NtrB enzyme through different pharmacophore groups. The effects of -Br and -NO_2 groups at different positions in phenylacetamide **(A1-A4)**, morpholine or piperidine heterocycles in **A5-A6**, -NO_2, -Cl, -CH_3, -$N(CH_3)_2$, -$N(n\text{-}Bu)_2$ functional groups at different positions in *N*-substituted phenylbenzamide **(A7-A14)** and two benzamide groups and various linkers such as -Et, -Bu as short/long alkyl chains, piperazine as a heterocyclic group, 1,2-, 1,3-, 1,4- cyclohexyl, phenyl as alicylic/aromatic rings at bis(4-nitrobenzamide) **(A15-A23)** were investigated. Herein, we report synthesis data, enzymatic and cytotoxic results of a series of nitro containing amide prodrugs with both experimental and *in silico* methods. Detailed structure-activity relationship (SAR) results were also discussed (Figure 2).

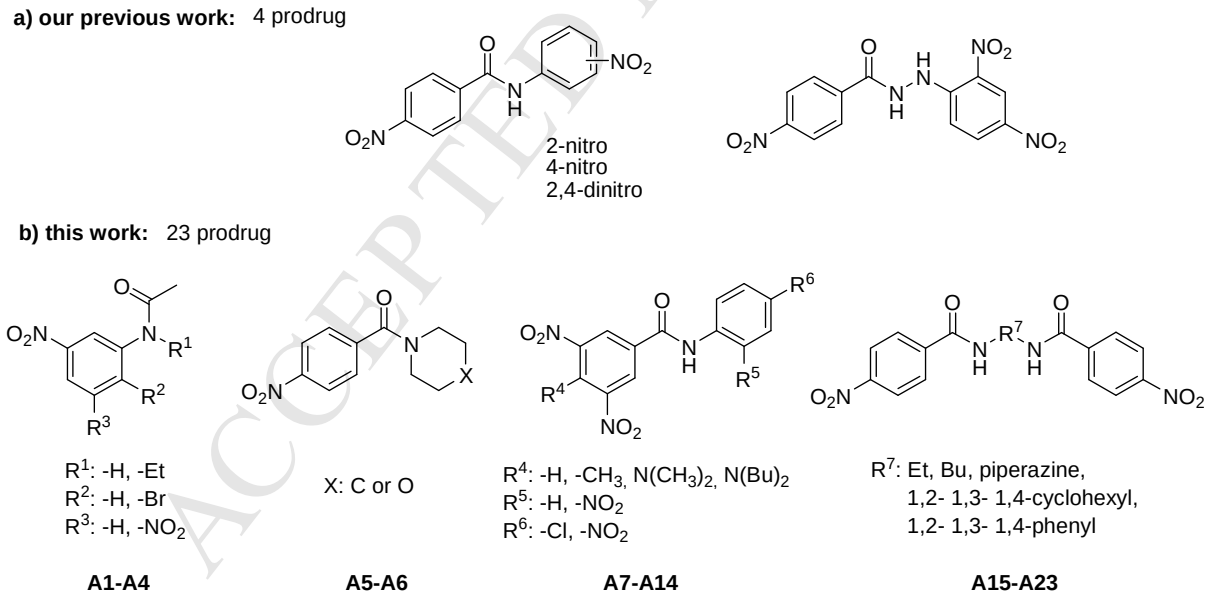

Figure 2. An overview of amide based prodrug structures studied (a) previously [39] and (b) in this work

2. RESULT AND DISCUSSION

2.1. Chemistry

All of the known products were confirmed by comparison of their spectral data with those reported in the literature. The prodrugs were fully characterized by their melting point, FT-IR, ^{1}H NMR, ^{13}C NMR and MS spectras.

A1 and **A3** prodrugs were synthesized from aniline derivatives *via* acetylation reaction in good yields 92% and 81%, respectively. Prodrugs **A2** and **A4** were obtained from **A1** or **A3** and ethyl iodide at the conditions that used NaH as base in DMF solvent at room temperature in 42 % and 82 % yields, respectively [40] (Figure 3).

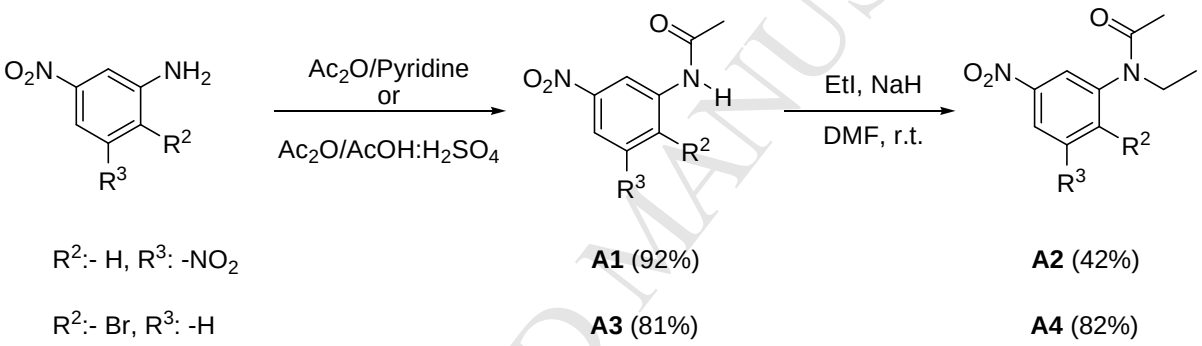

Figure 3. Synthesis of **A1-A4**

As revealed in Figures 4 and 5, different reaction conditions were applied to obtain **A5-A23** prodrugs by amidation reaction. Prodrugs **A7-A14** were synthesized from different aniline derivatives (4-chloroaniline, 4-nitroaniline and 2,4-dinitroaniline) and various 3,5-dinitrobenzoic acid derivatives that contain some functional groups like as -H, -CH_3, -$N(CH_3)_2$, -$N(n\text{-}Bu)_2$ at 4-position by using DCC and DMAP at Steglish esterification conditions (Figure 4).

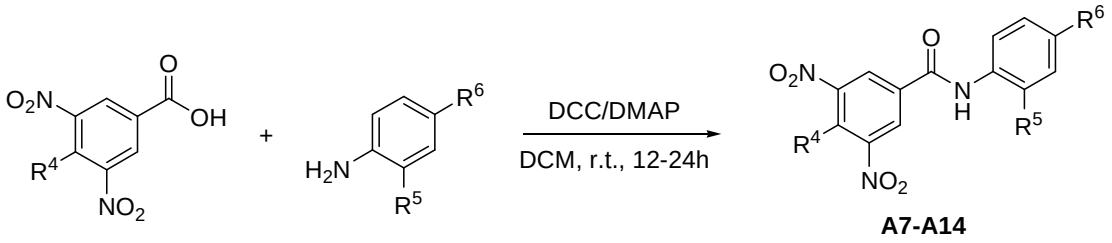

R^4: -H, R^5, R^6: $-NO_2$	**A7** (38%)
R^4: $-CH_3$, R^5:-H, R^6: $-NO_2$	**A8** (20%)
R^4: $-CH_3$, R^5, R^6: $-NO_2$	**A9** (48%)
R^4: $-N(CH_3)_2$, R^5:-H, R^6: -Cl	**A10** (74%)
R^4: $-N(CH_3)_2$, R^5:-H, R^6: $-NO_2$	**A11** (53%)
R^4: $-N(CH_3)_2$, R^5, R^6: $-NO_2$	**A12** (50%)
R^4: $-N(n\text{-}Bu)_2$, R^5:-H, R^6: -Cl	**A13** (79%)
R^4: $-N(n\text{-}Bu)_2$, R^5:-H, R^6: $-NO_2$	**A14** (67%)

Figure 4. Synthesis of **A7-A14**

A5 and **A6** were synthesized from 4-nitrobenzoyl chloride and piperidine **(A5)** or morpholine **(A6)** according to known methods with some modifications (Figure 5). Prodrugs **A15-A23** were obtained from 4-nitrobenzoyl chloride (1.0 equiv.) and various aliphatic, aromatic or heterocyclic diamino compounds (2.0 equiv. or more) at traditional conditions or by using microwave irradiation (Figure 5). Prodrugs **A15-A17** were prepared from 4-nitrobenzoyl chloride and diamino derivatives (ethylenediamine, 1,4-diaminobutane or piperazine) with triethylamine in DMF at room temperature or 50 ˚C for 5-6 h in moderate yields (Figure 5). Prodrugs **A18-A20** were synthesized by using 1,2-, 1,3- or 1,4-diaminocyclohexane with triethylamine in chloroform at reflux temperature for 8-14 h in 65-75% yields (Figure 5). Prodrugs **A21-A23** were obtained from 1,2-, 1,3- or 1,4-diaminobenzene with DMAP in pyridine at 70 °C by using microwave energy for 20-25 min (Figure 5).

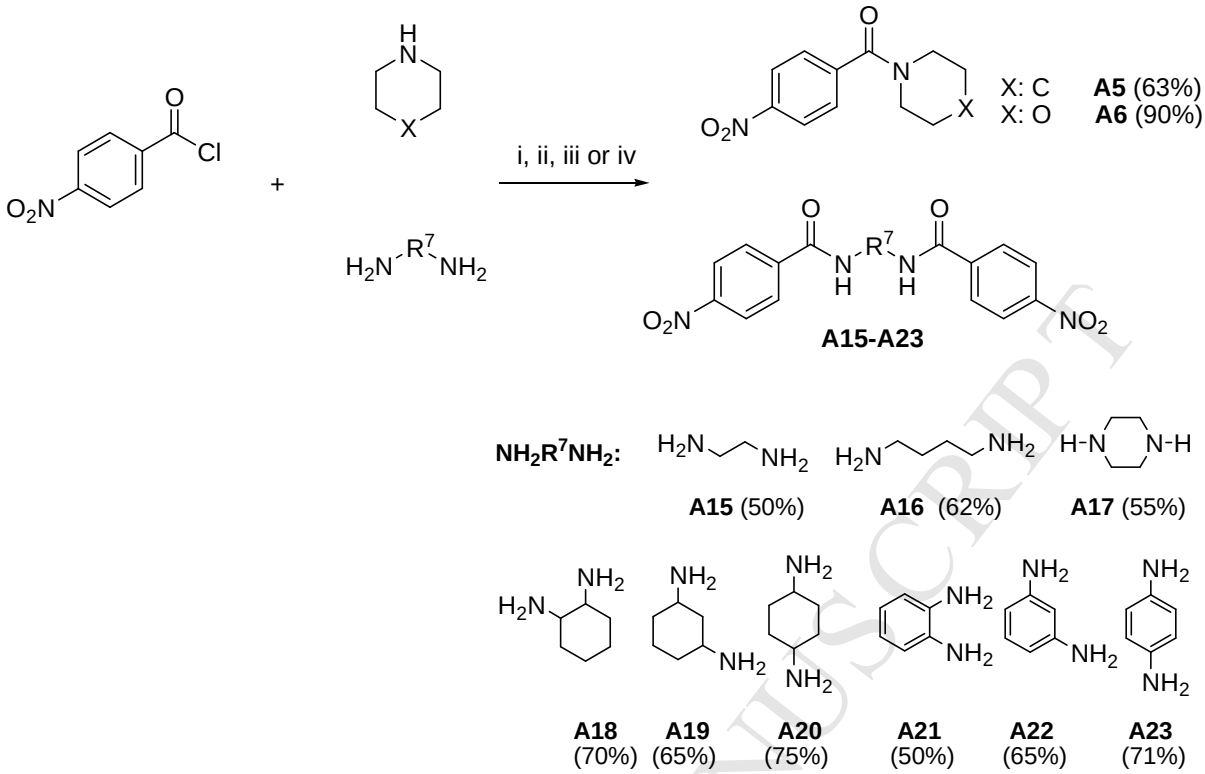

Figure 5. Synthesis of **A5, A6** and **A15-A23**

(i. K_2CO_3/MeCN/reflux/6h (for **A5**); ii. Et_3N/DCM/reflux/8h (for **A6**); iii. Et_3N/DMF/r.t or 50 °C/5-6h (for **A15-A17**); iv. $Et_3N/CHCl_3$/reflux/8-14h (for **A18-A20**); v. Microwave irradiation/DMAP/pyridine/70 °C/20-25 min (for **A21-A23**)

Many of the products (especially **A15-A23**) had very low solubility in common organic solvents resulting in difficulties at the purification steps of the corresponding products. Therefore, purification was carried out by crystallization or hot and/or cold washing with solvents that have different polarity.

2.2. *In silico* process

Generally, *in silico* methods including computational calculation and molecular modeling techniques are used to design and develop an overview and/or new solutions in biomedical applications. So those, *in silico* ADMET and molecular docking studies were performed to support the evaluation and illumination of this study.

2.2.1. ADMET studies

Understanding of ADMET properties of prodrug candidates are immensely essential process to solve or eliminate the undesired pharmacokinetics and toxicitiy effects. Therefore, the entitled compounds were selected and drug-like properties were determined according to Lipinski (rule of five) [41] and Veber rules, [42] (Table 1). Two compounds, **A13** and **A14** which are remarked as red color in Table 1 were removed from the data since they violated Veber and Lipinski rules. After this part, ADMET parameters were calculated by using DS 2017, [43] as given in Table 2. Additionally, ADMET plot was built by using calculated AlogP98 versus PSA_2D properties, indicating the confidence level of the predictions for the Blood Brain Barrier Penetration (BBB) model and the Human Intestinal Absorption (HIA) model (Figure 6). This plot represents the two analogous 95% and 99% confidence ellipses corresponding to HIA and BBB models. PSA value of any compound has an inverse relationship with human intestinal absorption value of any compound and so cell wall permeability [44]. AlogP98 is shown to lipophilicity the fact that this value is a raito, used to estimate hydrophilicity and ahydrophobicity. For this reason, the information of H-bonding characteristics as obtained by calculating PSA could be taken into consideration along with AlogP98 calculation [45]. The 95% confidence ellipse indicates the region of chemical space including well-absorbed compounds (≥90%). However 99% confidence ellipse demonstrates the region of chemical space that includes the compounds with excellent absorption through cell membrane. As it is well known, any compound with an optimum cell permeability should follow these criteria (PSA < 140 $Å^2$ and AlogP98 < 5) [45]. The compounds (**A1-A6, A10, A17, SN23862** and **CB1954**) showed polar surface area (PSA) < 140 $Å^2$, except compounds (**A7-A9, A11-A12, A15-A16** and **A18-A23**) that have also in turn violated the 99% and 95% confidence ellipse for both HIA and BBB (Figure 6). When we consider the AlogP98 criteria, all compounds had AlogP98 value <5. In Table 2, absorption level of most of the compounds

is 0 which indicates a very good human intestinal absorption except compounds (**A7-A9, A11-A12, A15,A16, A18-A23**) all have fallen outside the 99% absorption ellipse (level 2 and 3; poor or very poor). Compounds **SN23862, CB1954, A17** and **A10** also poses moderate HIA value, level 1. The aqueous solubility has an important role in the bioavailability of the optimal drugs, with the exception of compounds **A3-A6, A17, SN23862** and **CB1954** that had good aqueous solubility level (level 3) as referred in DS 2017, all other compounds had low but possible aqueous solubility levels such as level 2. Table 2 revealed that generality of the compounds had undefined values for BBB penetration with the exception of compounds **A2, A3, A4, A5** and **A6** that had medium BBB penetration level. On the other hand, all compounds had predicted hepatotoxicity values. Our results indicate that all compounds were found toxic to liver. Similarly, all ligands exhibited satisfactory effects with respect to CYP2D6 liver (with reference to DS 2017), suggesting that compounds are inhibitors of CYP2D6 (Table 2). This demonstrates that all studied compounds were not metabolized well in Phase-I metabolism. Finally, the ADMET plasma protein binding property prediction remarked that the compounds (**A1-A6, A10, A17, SN23862** and **CB1954**) had binding ≥ 90%, respectively, (refer to DS 2017), clearly suggesting that compounds (**A1-A6, A10, A17, SN23862** and **CB1954**) have good bioavailability and are highly bound to carrier proteins in the blood.

208 **Table 1.** The Lipinski and Veber rules analysis of the compounds (**A1-A23**) and reference compounds (CB1954 and SN23862) for Ssap-NtrB.

Comp.	AlogP (≤5)	MW (≤500 g/mol)	MPSA (≤140 A^2)	HA_Lipinski (≤10)	HD_Lipinski (≤5)	NRB (≤10)	HA_Veber (≤12)	HD_Veber (≤12)
A1	0.739	225.158	120.73	8	1	3	5	1
A2	1.293	253.211	111.94	8	0	4	5	0
A3	1.593	259.057	74.92	5	1	2	3	1
A4	2.147	287.11	66.13	5	0	3	3	0
A5	2.055	234.251	66.13	5	0	2	3	0
A6	0.826	236.224	75.36	6	0	2	4	0
A7	2.192	377.223	212.37	14	1	6	9	1
A8	2.784	346.252	166.55	11	1	5	7	1
A9	2.678	391.249	212.37	14	1	6	9	1
A10	3.23	364.741	123.97	9	1	5	6	1
A11	2.46	375.293	169.8	12	1	6	8	1
A12	2.354	420.291	215.61	15	1	7	10	1
A13	5.887	448.900	123.97	9	1	11	6	1
A14	5.117	459.452	169.8	12	1	12	8	1
A15	1.683	358.306	149.83	10	2	7	6	2
A16	2.326	386.359	149.83	10	2	9	6	2
A17	1.913	384.343	132.25	10	0	4	6	0
A18	3.114	412.396	149.83	10	2	6	6	2
A19	2.72	412.396	149.83	10	2	6	6	2

A20	2.844	412.396	149.83	10	2	6	6	2
A21	3.188	406.348	149.83	10	2	6	6	2
A22	3.188	406.348	149.83	10	2	6	6	2
A23	3.188	406.348	149.83	10	2	6	6	2
CB1954	0.601	252.184	137.73	9	2	4	6	1
SN23862	2.113	351.143	137.97	9	2	8	6	1

Footnote: Comp, compound; ALogP, octanol/water partition coefficient, a measure for lipophilicity; MW, molecular weight; MPSA, molecular polar surface area; HA_Lipinski, Number of hydrogen bond acceptors; HD_Lipinski, Num_H_Donors_Lipinski; Number of hydrogen bond donors; NRB, Number of Rotatable bonds; HA_Veber, Number of hydrogen bond acceptors based on Veber; HD_Veber, Number of hydrogen bond donors based on Veber.

Table 2. *In silico* ADMET analysis of the 21 compounds and reference compounds (CB1954 and SN23862) for Ssap-NtrB. The entitled compounds were divided into three parts and ordered from right to left and from top to bottom on the plot. The compounds (**A7-A9, A11-A12, A15-A16 and A18-A23**) outside of the all ellipses in the ADMET plot were colored grey. In the second part, compounds (**A1-A2, A10, A17, SN23862 and CB1954**) were colored blue. In the last part, compounds (**A3-A6**) inside of all ellipses in the graphic were shown red.

Comp.	PSA_2D(< 140 Å^2)	AlogP98(< 5)	HIA	Solubility	BBB	CYP2D6	Hepatotoxic	PPB
A1	115.757	0.739	0(good)	3(good)	4 (undefined)	false	true	true
A2	106.299	1.293	0(good)	3(good)	2(medium)	false	true	true
A3	72.934	1.593	0(good)	3(good)	2(medium)	false	true	true
A4	63.476	2.147	0(good)	3(good)	2(medium)	false	true	true
A5	63.476	2.055	0(good)	3(good)	2(medium)	false	true	true

A6	72.406	0.826	0(good)	3(good)	2 (medium)	false	true	true
A7	201.403	2.192	3 (very low)	2(low)	4(undefined)	false	true	false
A8	158.58	2.784	3 (very low)	2(low)	4(undefined)	false	true	false
A9	201.403	2.678	3 (very low)	2(low)	4(undefined)	false	true	false
A10	119.109	3.23	1 (moderate)	2(low)	4(undefined)	false	true	true
A11	161.932	2.46	3 (very low)	2(low)	4(undefined)	false	true	false
A12	204.755	2.354	3 (very low)	2(low)	4(undefined)	false	true	false
A15	145.868	1.683	2 (low)	3(good)	4(undefined)	false	true	false
A16	145.868	2.325	2 (low)	3(good)	4(undefined)	false	true	false
A17	126.952	1.914	1(moderate)	3(good)	4(undefined)	false	true	true
A18	145.868	3.114	2 (low)	2(low)	4(undefined)	false	true	false
A19	145.868	2.72	2 (low)	2(low)	4(undefined)	false	true	false
A20	145.868	2.844	2 (low)	2(low)	4(undefined)	false	true	false
A21	145.868	3.188	2 (low)	2(low)	4(undefined)	true	true	false
A22	145.868	3.188	2 (low)	2(low)	4(undefined)	true	true	false
A23	145.868	3.188	2 (low)	2(low)	4(undefined)	true	true	false
CB1954	132.839	0.601	1(moderate)	3(good)	4(undefined)	true	true	true
SN23862	132.839	2.113	1(moderate)	3(good)	4(undefined)	true	true	true

Abbreviations: PSA, polar surface area; AlogP98, the logarithm of the partition coefficient between n-octanol and water; HIA, Human Intestinal Absorption, BBB blood brain barrier; CYP2D6 cytochrome P450 2D6 binding, false for CYP2D6: non-inhibitor; True for Hepatotoxic: toxic; PPB plasma protein binding, more than 90% for PPB value is true: Chemicals strongly bound. Less than 90% for PPB value is false: Chemicals weakly bound.

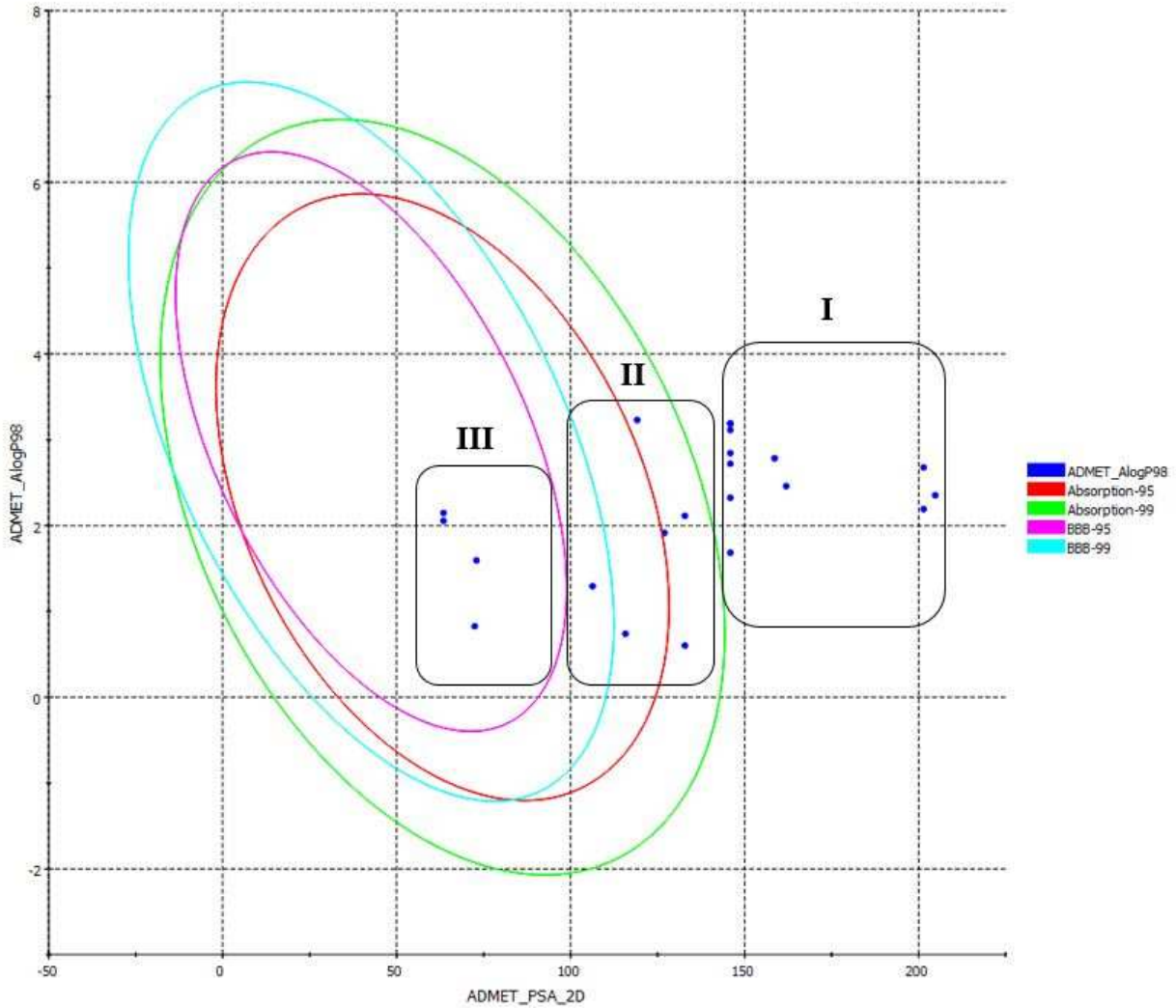

Figure 6. ADMET plot for various nitro amide derivatives as anticancer prodrugs

2.2.2. Molecular docking results

According to the biological activity studies and ADMET analysis, the selected five compounds (**A2, A5, A6, A17** and **A20**) were docked with Ssap-NtrB model. In the meantime, CB1954 and SN23862 as reference compounds were redocked with Ssap-NtrB model which was modelled in our previous study [39]. The results of redocking revealed that obtained results were compatible with the literature [18, 39].

Based on the redocking process, molecular docking was applied between the chosen three compounds and Ssap-NtrB model. To clarify the binding forms of the chosen compounds, binding affinities were also predicted by using molecular docking. Furthermore, interactions of each compound-enzyme complex were defined and the interactions that are dominant or not in active site of the enzyme model were specified. As shown in Figure 7, Compound **A5** formed two hydrogen bonds with A: Arg13 (2.068 Å), B: Ser43 (1.89 Å) and one hydrophobic interaction with FMN (4.34 Å). On the other hand, compound **A6** was shown to have also same interactions with compound **A5** except that the same nitro group in compound **A6** showed hydrogen bond interaction with B: Val44 instead of B: Ser43 residue of the enzyme. The compound **A2** has a similar interaction with SN23862 as the reference compound. The other ones, **A17** and **A20** have different framework than others, but bound on the active site of the enzyme. Compound **A17** formed two hydrogen bond with B: Ser43 (2.79 Å), B: Pro41 (2.75 Å) and one π-π stacking with FMN like compound **A5**. However, it was shown to have unfavorable interactions with A: Phe162, A: Val204 and B: Pro41 residues that are displayed as red dash line and spheres in Figure 7. The last compound **A20** was shown to have hydrogen bonds and hydrophobic interactions with different residues of the binding site in Ssap-NtrB. It was also observed that prodrug **A2**, **A5** and **A20** formed stronger hydrophobic interactions with hydrophobic pocket than other compounds **A6** and **A17**. The binding forms are demonstrated that the para nitro and carbonyl groups in phenyl ring were

264 able to affect the interaction on Ssap-NtrB significantly. Interaction types and distances of the

265 studied compounds and standard prodrugs were given in SI-Table S1.

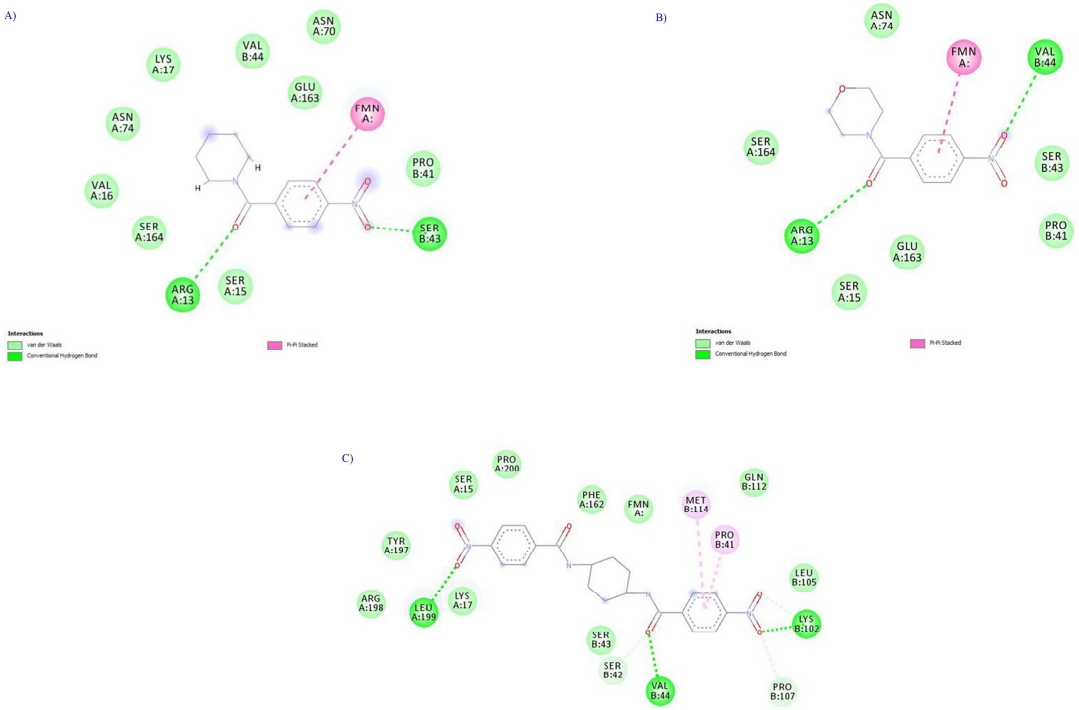

Figure 7. Two-dimensional docking poses of compound **A5** (**A**); compound **A6** (**B**); compound **A20** (**C**) in the binding site of Ssap-NtrB *Hydrogen bonds were shown with yellow dash lines and dark green spheres. The pink sphere and dash lines presented cofactor FMN and pi-pi stacked.The hydrophobic interactions which is van der Waals were represented by light green spheres. Unfavorable interactions like steric bumps were displayed as red dash line and spheres.

Additionally, binding energy (ΔG) and inhibition constant (Ki) values of the compounds were computed using DS 2017 program are represented in Table 3. The molecular docking results showed that compounds **A5, A17 and A20** displayed lower binding energy values and higher affinities for target enzyme than did CB1954 and SN23862. Topological polar surface area (TPSA) [46] and AlogP [47] of each compound was also computed using DS 2017 demonstrating the membrane permeability and lipophilicity of the compounds, respectively. The results are exhibited in Table 3. These parameters are very important properties for drug discovery. If TPSA value is greater than 140 $Å^2$, a compound has no enough level for membrane permeability. The obtained values of the compounds (152.959-257.443) except **A5** (130.459) are greater than 140 $Å^2$. These results reveal that **A5** compound can be a suitable prodrug, having hydrophobic property, good membrane permeability and specifically targeting Ssap-NtrB.

Table 3. The binding energy (ΔG), inhibition constant (Ki), Topological polar surface area (TPSA) and ALogP values of the compounds and CB1954 and SN23862 as standard prodrugs with that of Ssap-NtrB.

Prodrugs	ΔG (kcal/mol)	Ki (μM)	TPSA	AlogP
A2	-6.98	7.67	224.312	1.293
A5	-7.56	2.85	130.459	2.055
A6	-6.88	9.06	152.959	0.826
A17	-7.95	1.49	257.443	1.913
A20	-7.05	6.82	253.935	2.844
CB1954	-7.13	5.96	213.711	0.601
SN23862	-7.01	7.28	195.360	2.113

2.3. Enzymatic reduction via Ssap-NtrB

2.3.1. Metabolite profiles of prodrugs A1-A23

Initial activation screening of all synthesized amide prodrugs **A1-A23** by Ssap-NtrB was performed in accordance with the assay condition described in the experimental section. Reduction profiles of the prodrugs **A1-A23** were assessed according to HPLC chromatograms.

All the prodrugs except **A10, A13-A14, A16-A17** and **A20-A23** were readily reduced by Ssap-NtrB with half-lives of up to 3 hours. However, there were some product formation upon longer reaction times of **A10, A13-A14, A17** and **A20-A21** with Ssap-NtrB in cofactor regeneration system (Table 4).

Table 4. Ssap-NtrB activation of compounds **A1-A23**

Compound	Retention time (min)	Half life $t_{1/2}$ (h)*	Amount of product after 10 min (%)**	Retention times of major metabolites (min)	HPLC program ***
A1	14.4	< 0.1	88	8.15, 12.06, 15.84	I
A2	14.55	<0.02	100	11.65	I
	16.85	<0.02	100	11.8, 14.2	II
A3	13.88	< 0.2	56.4	7.12, 15.74	I
A4	15.18	< 0.1	78	12.28, 15.55, 18.39	I
A5	18.22	< 1.5	5.57	15.99	I
	17.81	<0.02	100	14	II
A6	15.17	< 0.25	65.4	11.71	I

A7	14.51, 17.52	<0.37	23	9.76	I
A8	18.04	< 0.38	22	15.94	I
	23.93	< 0.26	32.96	20.16, 20.79	II
A9	18.07	< 0.23	36.6	14.45, 17.61, 15.35	I
	24.11	< 0.18	48	17.44, 21.6, 23.88	II
A10	19.22	-	-	-	I
	25.86	< 3.15	2.65	17.02, 20.14, 22.67	II
A11	18.43	< 0.3	28	15.83, 16.24, 16.84	I
A12	18.51	< 0.42	20.3	2.97, 11.5	I
	24.85	< 0.1	90.1	12.04, 19.19, 21.58	II
A13	20.12	-	-	-	I
	34,2	< 2.4	3.6	29.05	II
A14	26.5	-	-	-	I
	31.96	< 1.56	5.34	28.34	II
A15	17.56	< 2.54	6.57	10.39, 14.06	II
	18.65	< 1.2	7.2	15.8	I
A16	19.02	-	-	-	I
	17.28	-	-	-	I

A17	17.6	< 1.42	5.9	11.53, 14.47, 14.85	II
A18	20.85	< 1.8	9.33	15.55, 17.99, 17.7	II
	20.91	< 0.52	16.2	19.43	I
A19	19.40, 20.15	< 0.26	32.7	14.03, 14.58, 16.83, 17.4	II
	19.44, 20.6	< 2	4.25	17.87	I
A20	19.96	-	-	-	I
	19.2	< 1.5	11.2	13.48	II
A21	22.08	< 3.2	5.25	16.49	II
	21.38	-	-	-	I
A22	21.98	-	-	-	II
	21.88	-	-	-	I
A23	16.61	-	-	-	I

**approximate time needed for reduction of the substrate amount up to 50% upon Ssap-NtrB activation.*
***Percent of products produced upon reduction of the substrate by Ssap-NtrB (initial amount of substrate was taken as 100%). In a typical solution, 50-100 µM substrate was dissolved in 25 mM, pH 7.5 Tris/Cl buffer with 5-10% DMSO concentration and incubated with NADH (200-500 µM) and Ssap-NtrB (2.5-30 ug/mL) at 21-25°C. The amounts were calculated from the HPLC chromatogram peak areas as a function of time.*
**** HPLC program I: 0-5 min at 20% ACN, 15-22 min at 80% ACN, 27-32 min at 20% ACN*
HPLC program II: 0-5 min at 20% ACN, 25-35 min at 80% ACN, 40-45 min at 20% ACN, used for coupled reaction analysis.

A2, A5, A7-A10, A12-A15, A17-A22 reactions with Ssap-NtrB were monitored against time by using cofactor regeneration system with recombinant formate dehydrogenase (FDH) from *Candida methylica* (CmFDH) (Figure S59). In cofactor regeneration system reactions, the FDH enzyme converts NAD to NADH, thus sufficient amount of NADH will be available

for nitroreductase reduction reactions. By this coupled enzyme system (Ssap-NtrB and FDH), the time dependent profile of reactions can be monitored for longer periods without the limititation of the cofactor since Ssap-NtrB is a NAD(P)H dependent enzyme and needs NAD(P)H in order to convert the substrate into its products.

HPLC results indicated that **A2, A5, A6** and **A19** were faster reduced by Ssap-NtrB while **A2** was the fastest reduced substrate by Ssap-NtrB with only around one minute half-life. 100% conversion of the parent compound were observed in **A2**/Ssap-NtrB reaction and **A5**/Ssap-NtrB coupled reaction involving cofactor regeneration (Table 4). For **A2**/Ssap-NtrB reaction, multiple product peaks were detected at 11.8 min and 14.2 min after coupled reaction while only one product were detected from the reduction reaction with limited amount of cofactor (Fig. 8 and SI). Similarly, there were two metabolites produced upon **A5** /Ssap-NtrB-FDH coupled reaction since there was only one metabolite produced after 10 minutes of reaction with limited NADH. This states that the amount of NADH was not sufficient for the reduction reaction to take place until the last step. However, when there was enough cofactor, all the **A5** substrate (100%) was reduced to its metabolites (14.0 and 22.3 min retention times).

The product profiles of reduction reactions exhibited time-dependent properties. As an example, the release of products from Ssap-NtrB/**A2** reaction as a function of time is shown in Figure 8. Products' profiles versus time shown in Figure 8B and 8C indicated that five products were observed after enzymatic reduction with retention times of 11.8 min, 14.2 min, 21.2 min, 8.0 min and 15.2 min. At the end of 2 min reaction time, all of the product **A2** was converted to corresponding metabolites. The main product P1 formation increased with time upon the increased production of P2 product. At the end of 30 min, there were no P1 and P3 products stable, predicted to be converted to prodrugs P4 and P5.

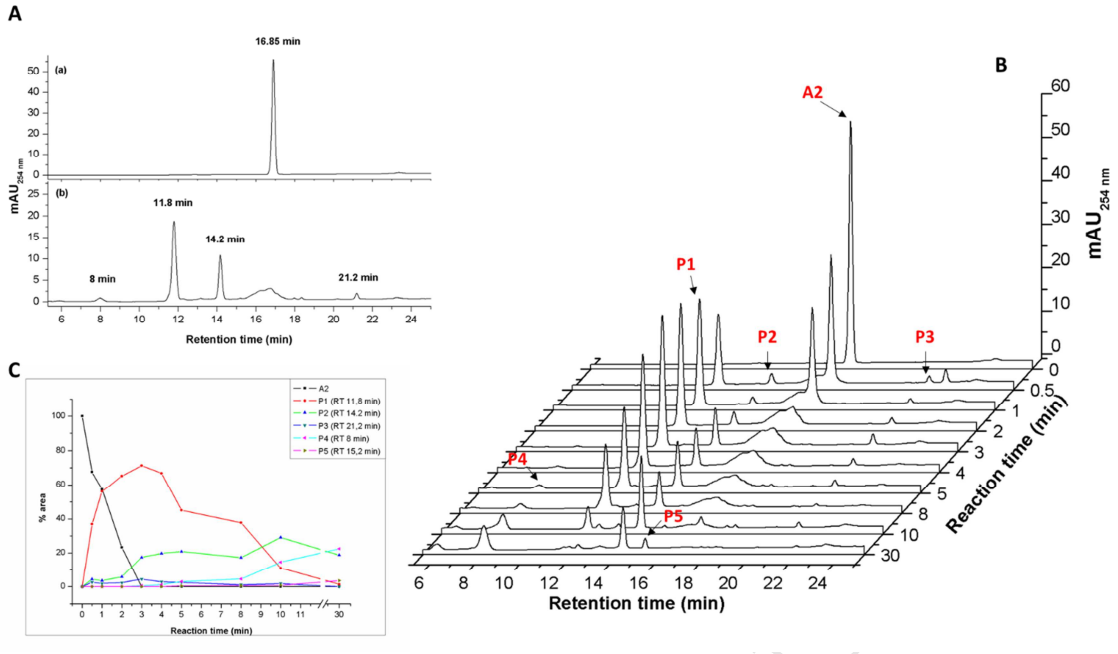

Figure 8. A) HPLC chromatogram of reduction reaction of prodrug **A2** catalyzed by Ssap-NtrB, (a) Control without Ssap-NtrB, (b) Enzymatic reduction reaction at 5 min, (B) HPLC chromatogram of reactions, (C) Time dependent product profiles.

Aromatic nitro compounds have been indicated to be reduced by different nitroreductases [48]. Dinitrobenzamide derivatives such as CB1954 and derivatives, SN23862 and PR-104 [24, 25, 26] have been approved to be effective against different nitroreductases especially *E. coli* nitroreductases. In this study, nitroaromatic prodrug candidates **A1-A23** were synthesized and their probability of reduction by a different nitroreductase (Ssap-NtrB) was examined. Among amide derivatives, **A1-A9, A11-A12, A15** and **A18-A19** compounds were easily reduced while Ssap-NtrB was not reactive for **A16, A22** and **A23** compounds even after long reaction times with cofactor regeneration system.

2.3.2. Kinetic studies

Due to low solubility of the compounds, not all compounds were able to be assessed to undergo reduction with Ssap-NtrB. Steady-state kinetic experiments were performed for compounds **A1** and **A2** with calculating specific activities of a range of prodrug concentrations (0-800 µM) dissolved in 5% DMSO. Catalytic efficiencies (k_{cat}/K_M) of Ssap-

NtrB with **A1** and **A2** were calculated as 98284 s^{-1} M^{-1} and 117278 s^{-1} M^{-1} respectively. When compared with the catalytic activity of well-known CB1954/*E.coli* NfsB combination, Ssap-NtrB/**A1** and Ssap-NtrB/**A2** were found to be much more effective (17.55 and 20.94 fold respectively) representing to be better NTR/prodrug combinations for cancer therapy (Table 5). In addition, the catalytic efficiencies of our NTR/prodrug combinations are higher than the NfsB/PR-104A combination, which was found to be more effective alternative prodrug than CB1954 [19].

Since there are many mechanisms of reduction in the living cells, it is not possible to assess all enzymatic reduction modes *in vitro* in tubes. Thus, further *in vitro* cell culture experiments were conducted in order to see the effect of prodrugs and reduction products in cancer cell lines.

Table 5. Comparison of kinetic parameters of nitroreductases toward CB1954, SN23862 and prodrugs **A1-A23**

Enzyme	Substrate	k_{cat} (s^{-1})	K_M (μM)	k_{cat}/K_M (s^{-1} M^{-1})	Relative to CB1954/NfsB	Cofactor
NfsB	CB1954	62 ± 11	11000 ± 2600	5600	1	NADH
NfsB	SN23862	26.4 ± 7.2	2500 ± 100	10560	1.89	NADH
NfsB	PR-104A	60	4500	13000 ±7800	2.32	NADH
Ssap-NtrB	CB1954	2.26 ± 0.07	1065.2 ± 53.1	2120	0.38	NADPH
Ssap-NtrB	SN23862	0.8 ± 0.1	82.4±16.9	9350	1.67	NADPH
Ssap-NtrB	A1	9.9 ± 0.7	100.6 ±17.2	98284	17.55	NADPH
Ssap-NtrB	A2	1.37 ± 1.1	96.9 ± 21.4	117278	20.94	NADPH

2.4. Cytotoxic activity

2.4.1. Growth inhibitory effects of amides

Prodrug candidates were evaluated for cytotoxic properties against to Human Hepatoma (Hep3B), Human Prostate Cancer (PC3) cells and Human Umbilical Vein (HUVEC) cells as a healthy control model. The cells were treated with five different concentrations (150, 75, 39,

18 and 9 µM) of prodrugs and exposed for 48h. After 48h exposure, the cell viability results were obtained by using MTT method. % cell viability was calculated using spectrophotometric absorbance value at 550 nm wavelength. The results were divided into three groups: NT: Not Toxic (% Cell viability value > 80%; LT: Low Toxic (80% > % cell viability value > 51%) and T: Toxic (% Cell viability value < 50%). For toxic compounds, IC_{50} (50 % inhibition concentration) value was determined using Origin pro 8.5 program.

As shown in Table 6, **A1, A3-A6, A8, A11** and **A16-A22** were not toxic; **A2, A9, A15,** and **A23** were low toxic; **A7, A10** and **A12-A14** were toxic with 51.76 µM, 110.64 µM, 43.74 µM, 11.62 µM and 30.87 µM of IC_{50} values, respectively against Hep3B cells. For HUVEC cells, especially **A13** and **A14** were toxic with 22.60 µM and 22.24 µM of 50% inhibition concentration. **A7** and **A10** were low toxic. The rest of the compounds showed no toxic effect against HUVEC cells as chosen a healthy model. **A10, A13,** and **A14** compounds inhibited 50% cell proliferation as indicated concentrations 43.23 µM, 17.10 µM and 19.73 µM, respectively for PC3 cells. **A17** and **A19** were low toxic on PC3 cells.

The cytotoxicity results of the toxic compounds **(A7, A10** and **A12-A14)** are given in Figure 9. The rest of results are represented in SI-Figure S60.

Table 6. Growth inhibitory effects of prodrugs at concentration range between 150-9 µM (NT* referred as not toxic (% Cell viability value>80%). LT* referred as low toxic (80%> % cell viability value>51). T* referred as Toxic. (50% < % Cell viability value).

	Cytotoxic properties (IC_{50}-µM)		
Prodrugs	**Hep3B**	**HUVEC**	**PC3**
A1	NT	NT	NT
A2	LT	NT	NT
A3	NT	NT	NT

A4	NT	NT	NT
A5	NT	NT	NT
A6	NT	NT	NT
A7	**T (51.16 µM)**	**LT**	**NT**
A8	NT	NT	NT
A9	LT	NT	NT
A10	**T (119.64 µM)**	**LT**	**T (43.23 µM)**
A11	NT	NT	NT
A12	**T (43.74 µM)**	**NT**	**NT**
A13	**T (11.62 µM)**	**T (22.60 µM)**	**T (17.10 µM)**
A14	**T (30.87 µM)**	**T (22.24 µM)**	**T (19.73 µM)**
A15	LT	NT	NT
A16	NT	NT	NT
A17	NT	NT	LT
A18	NT	NT	NT
A19	NT	NT	LT
A20	NT	NT	NT
A21	NT	NT	NT
A22	NT	NT	NT
A23	LT	NT	NT

406

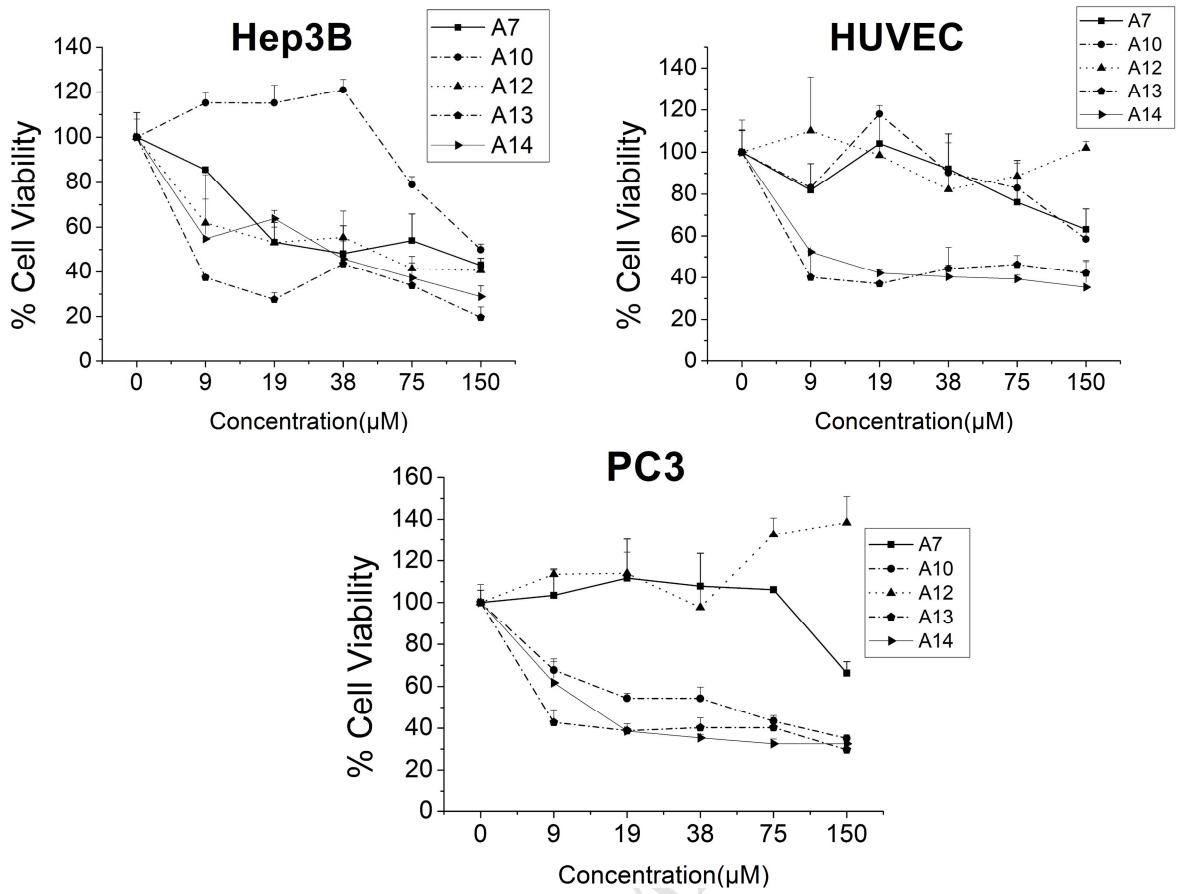

407

408 **Figure 9.** The cytotoxic properties of prodrugs (**A7, A10** and **A12-A14**) were determined
409 using MTT assay against Hep3B, PC3 and HUVEC cells. 50.000 cells/well were plated out in
410 96 well plates. Compounds were applied on plates at five different concentrations (9, 18, 39,
411 78, 150 µM). DMSO (1%) was used as vehicle control. After 48 h incubation, MTT assay was
412 carried out as described in ref 49. The results were obtained using spectrophotometer at 550
413 nm optic density. The graphics were illustrated using Origin pro 8.5 program.

414

415 **2.4.2. The prodrug abilities of nitro aromatic amides**

416 Compounds were chosen according to cytotoxic properties. Prodrug ability was searched
417 for nontoxic compounds. Hence, Ssap-NtrB/prodrug (**A1-A6, A8, A11** and **A15-A22**)
418 combinations were applied on PC3 cells. Also, CB1954, previously known to be a suitable
419 substrate for *E.coli* nitroreductase was used as a positive control to compare the prodrug
420 ability of compounds.

In this experimental design, the cells were treated with prodrug as NTR- (alone/180 nM at final concentration) and prodrug (three different concentrations of 180, 18 and 1.8 nM) +NADH(cofactor)+extracellular Ssap-NTR in 25mM Tris-HCl pH 7.5. After 48h of treatment, the growth inhibitory effects of combinations were analyzed using SRB method. Previously, it was determined that NADH had no toxic effect for PC3 cells (Data not shown). The IC_{50} values of amides with Ssap-NtrB (prodrug+NADH+Ssap-NTR) were shown in Table 7.

Our results indicated that **A5, A6** and **A20** were potential candidates as a prodrug. Combinations with Ssap-NtrB of these prodrugs, which were not toxic alone, have shown significant toxic effects. For these prodrugs, IC_{50} values were 1.806 nM, 1.808 nM and 1.793 nM, respectively (Figure 10). In addition, prodrug **A20** had toxic effect comparable with CB1954. The rest of the graphics of compounds were shown in SI-Figure 61.

Table 7. The prodrug abilities of amides. NTR (-) represents only 150 µM or 180 nM prodrug application. NTR (+) are values obtained from the application of final products of nitroaromatic amides/Ssap-NtrB reaction.

	Prostate cancer cell line (PC3)	
Prodrugs	***NTR(-)***	***NTR(+) IC_{50} value***
A1	*non toxic*	*10.72 µM*
A3	*non toxic*	*10.24 µM*
A4	*non toxic*	*12.59 µM*
A5	*non toxic*	***1.806 nM***
A6	*non toxic*	***1.808 nM***
A8	*non toxic*	*17.11 µM*
A11	*non toxic*	*29.12 µM*

A15	*non toxic*	*31.10 nM*
A16	*non toxic*	*36.83 nM*
A17	*non toxic*	*17.98 nM*
A18	*non toxic*	*15.47 nM*
A19	*non toxic*	*30.50 nM*
A20	*non toxic*	***1.793 nM***
A21	*non toxic*	*14.30 nM*
A22	*non toxic*	*33.43 nM*
CB1954	*non toxic*	***1.792 nM***

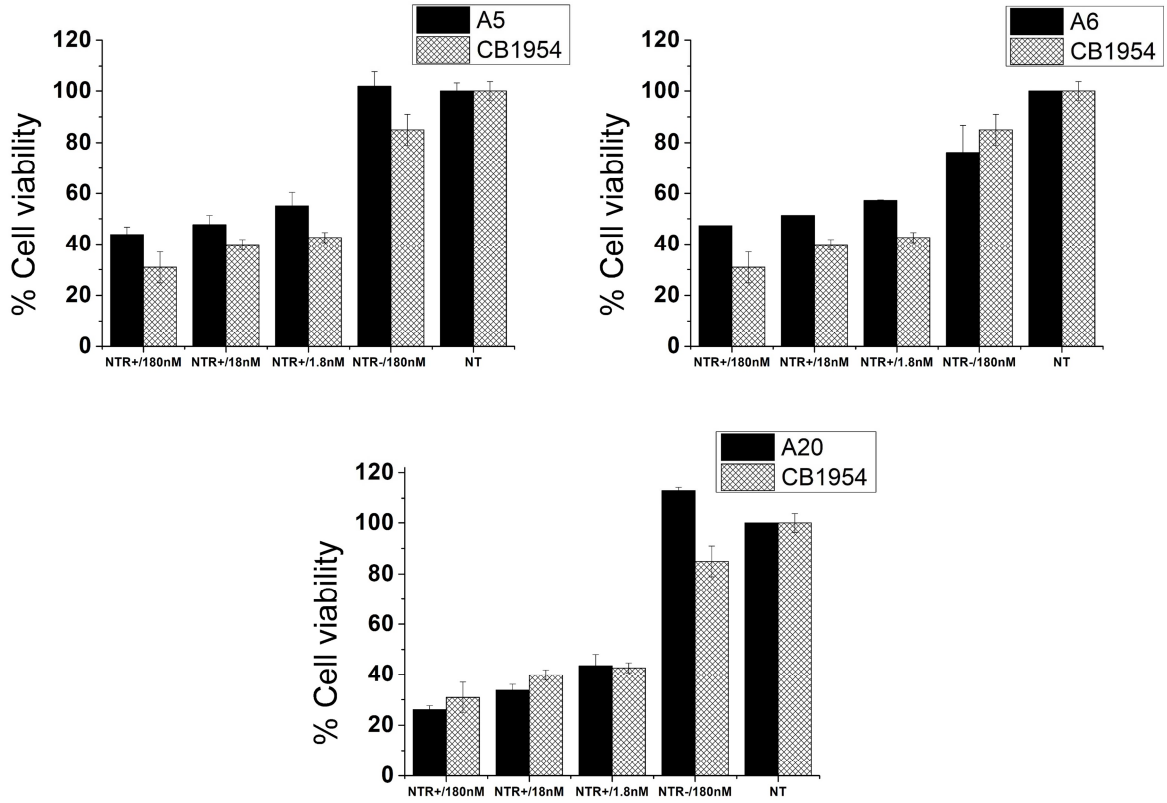

Figure 10. The prodrug abilities of amides were determined using SRB assay in PC3 cells. Cells were plated out in 96 plates 10.000 cells per well. C1 represented as control group of 180 nM final concentration amides alone. NT (Not Treated) was represented as vehicle control which the wells were treated with 25 mM Tris-HCl buffer. The combinations of Ssap-NtrB/Prodrug (R-180 nM, R-18 nM and R-1.8 nM) that were supplemented with NADH cofactor in 25 mM Tris-HCl were referred as R (Reaction) in graphics. After 48h of incubation with these combinations, results were obtained using spectrophotometer at 498 nm wavelength. Experiments were performed in three replicates. % SD values and % cell viability were calculated using Microsoft Excel program.

2.5. Structure-Activity Relationships (SARs)

Based on the results of ADMET and molecular docking studies, enzymatic and cytotoxicity experiments the preliminary SARs were characterized (Figure 11). According to

the PSA values, BBB and HIA model at ADMET studies, **A1-A6, A10** and **A17** compounds showed optimum cell permeability, good bioavailability and good binding properties.

It was observed that compound **A2, A5** and **A20** formed a stronger hydrophobic interactions with the hydrophobic pocket of the enzyme.

While small molecules such as **A2-A4** (*N*-(substitutedphenyl)acetamide derivatives) and **A6** (4-(4-nitrobenzoyl)morpholine) were reduced by Ssap-NtrB and produced metabolites fastly at limited cofactor system, compounds **A2, A5, A9** and **A12** were reacted with enzyme fastly at the regenerated system (Figure 11).

Among *N*-(substitutedphenyl)-3,5-dinitrobenzamides (**A7-A14)**, prodrug candidate **A13** and **A14** contain -N(n-Bu)$_2$ at 4-position of benzene ring were not obeying Veber and Lipinski rules unlike bearing -H, -CH_3, -N(CH_3)$_2$, at the same position. **A7, A10** and **A12-A14** derivatives in this series showed toxic effects on PC3 and Hep3B cells. We determined that **A13** and **A14** compounds are also toxic against HUVEC healthy cell model. So these compounds were eliminated to become a prodrug. IC_{50} values of the metabolites of other compounds (**A8** and **A11**) that have -CH_3, -N(CH_3)$_2$ at R^4 position and nitro group at R^6 position in this series are in the range of 17-30 µM.

Among *N*-(substitutedphenyl)acetamides (**A1-A4**), compound **A2** was observed to be low toxic against Hep3B cells. The metabolites of other compounds have IC_{50} values in the range of 10-13 µM.

When prodrug abilities of **A15-A23** compounds were evaluated, **A23** was determined as low toxic against Hep3B cells. The metabolites of other compounds (**A15-A22**) have IC_{50} values in the range of 14-37 nM. Prodrug candidates of these series have smaller, more advantageous IC_{50} values compare to acetamide derivatives (**A1-A4**) and *N*-(substituted phenyl)-3,5-dinitrobenzamides (**A7-A14)**.

IC_{50} values of **A5** and **A6** metabolites were found as 1.806 nM, 1.808 nM, respectively. These two compounds are 4-nitrobenzamide derivatives of piperidine and morpholine. To the best of our knowledge, although the synthesis of **A5, A6** at various experimental conditions is known in the literature, there was no evidence related to nitroreductase interaction of these compounds. IC_{50} value of metabolites of *N*,*N*'-(1,4-cyclohexyl)bis(4-nitrobenzamide) (**A20**) is 1.793 nM. The common points of three nitrobenzamide compounds (**A5, A6** and **A20**) are to have one or two nitro group (**A20** is a symmetrical molecule that have two nitro) and to be a benzamide derivative of nitrogen containing heterocyclic group such as piperidine, morpholine and piperazine. As a result of all the experiment, **A5, A6** and **A20** can be recommended as potential prodrugs to be used for NTR based cancer therapy (Figure 11).

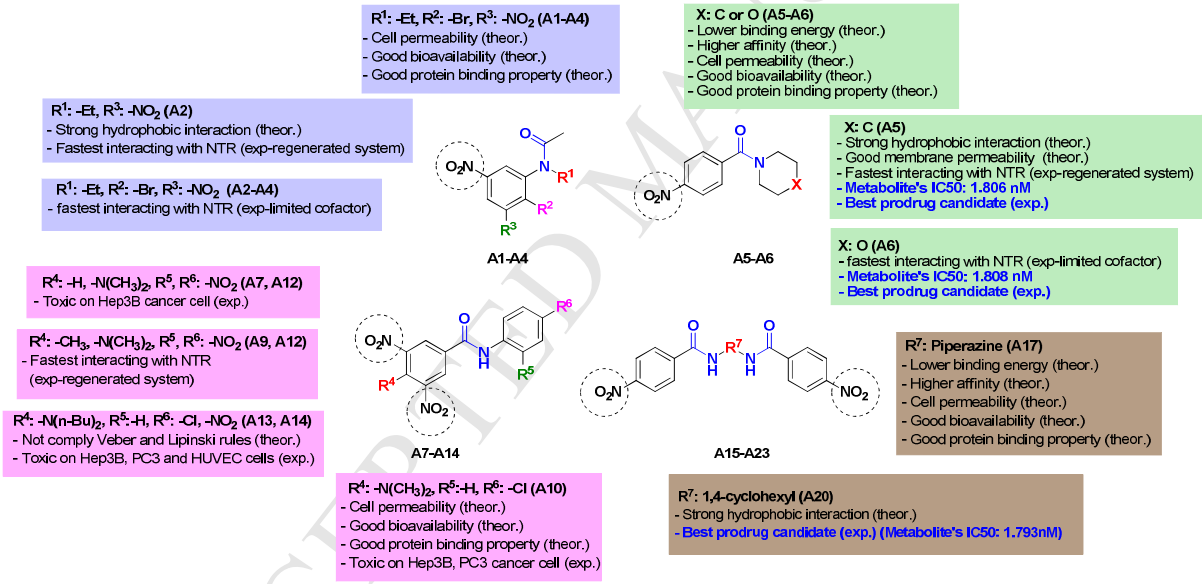

Figure 11. Structure-activity relationship (SAR) analysis of the amide prodrugs.

(theor.: according to theoretical results; exp: according to experimental results)

2.6. Metabolite profiles of prodrugs A5, A6 and A20

It is well known that when nitro bearing organic compounds interact with nitroreductase enzyme, nitro group converts to corresponding nitroso-unstable-, hydroxyl amine and amine metabolites, respectively. Accordingly, **A5** and **A6** prodrugs that contain one nitro group must

have two metobolites, hydroxylamine and amino (Figure 12A and 12B). According to HPLC chromatograms at Figure S58 and S59, while only hydroxyl amine metabolite (RT: 15.99 min) was occured at the 15 min reduction reaction of prodrug **A5** catalyzed by Ssap-NtrB, major hydroxylamine (RT: 14.0 min-more polar product) and minor amine (RT: 22.3 min-less polar product) metabolites were obtained at the catalysis of Ssap-NtrB and Cm-FDH cofactor regeneration conditions. Similarly, single hydroxylamine metabolite (RT: 11.71 min) of prodrug **A6** was determined by HPLC chromatogram of 15 min catalytic reaction with Ssap-NtrB (Figure S58). Prodrug **A20** have four possible metabolites (nitro-hydroxylamine, two hydroxylamine, hydroxylamine-amino, two amino) since it contains two nitro group (Figure 12C). According to experimental data, while no product formation was observed at 15 min Ssap-NtrB catalytic conditions because of limited enzyme and reaction time, three minor metabolites and one major metabolite (RT: 13.48 min) of **A20** were determined at cofactor regeneration system (Figure S58-S59).

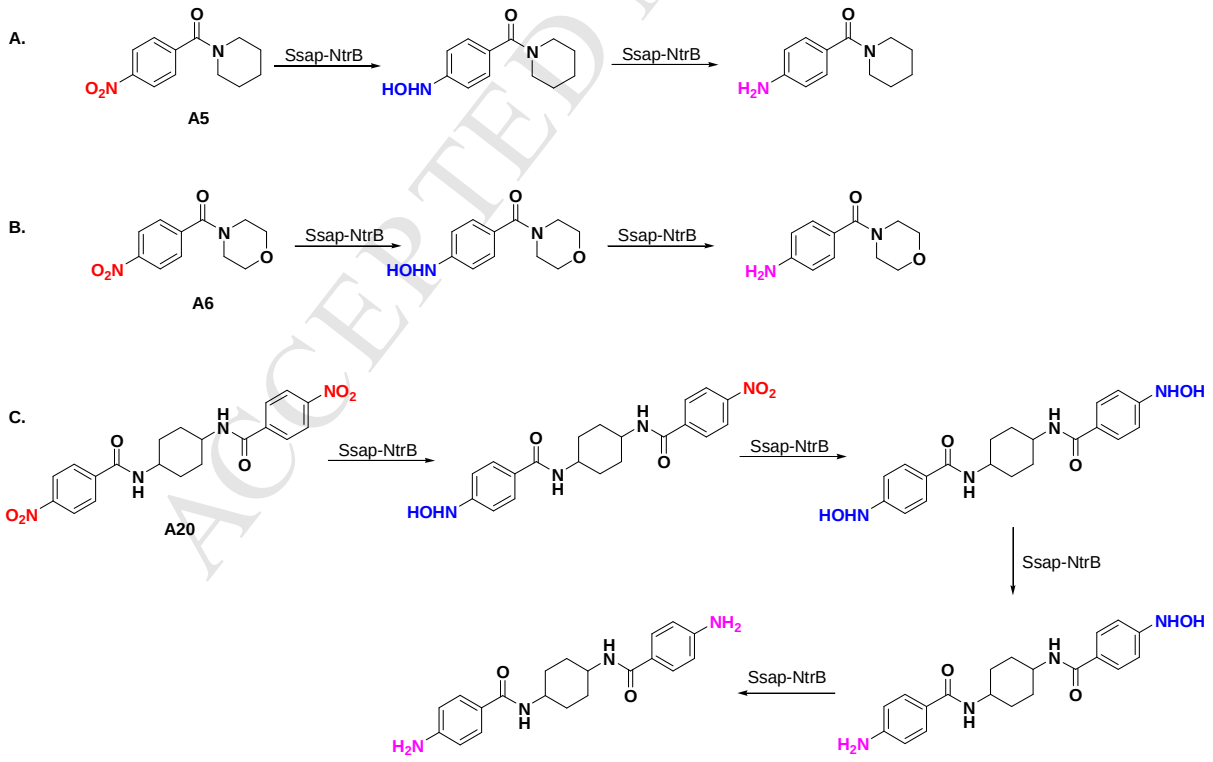

Figure 12. A5 (A), **A6** (B) and **A20** (C) prodrugs and their possible metabolites

3. CONCLUSION

In this study, we have synthesized and characterized 23 (twenty-three) aromatic amide compounds by using different reaction conditions, in moderate-good yields. 9 compounds **(A2, A4, A8-A14)** were newly synthesized in this study and 14 compounds were previously known in the literature. This study consisted of three steps. The first step, within the scope of theoretical studies, *in silico* ADMET and molecular docking analyses were performed. With *in silico* ADMET studies, pharmacokinetic, toxicity features and suitability for BBB and HIA models of prodrug candidates were determined. Molecular docking studies were carried out for five compounds which were selected from biological activities. Binding forms and binding affinities of these compounds were revealed. In the next step, enzymatic reduction reactions with Ssap-NtrB were achieved using HPLC analyses. Thirdly, biological activities of the compounds and the metabolites produced after Ssap-NtrB reactions were measured for assessing their cytotoxic properties on two different cancer cell lines. Prodrug toxicities were examined on both Hep3B and PC3 cells, than metabolite toxicities of the prodrugs that were found to be nontoxic in HUVEC cells were examined on prostate cancer cells.

In the theoretical part, ADMETox analysis showed that especially **A3-A6** compounds are more effective on NTR based cancer therapy. In molecular docking studies revealed that the synthesized compound **A5** for Ssap-NtrB has relatively optimal Binding Energy (-7.56 kcal/mol), TPSA (130.459 $Å^2$) and logP (2.055) values as compared to others. The results obtained from the docking process also supported the *in vitro* activity values. This study shows us not only interactions of nitro aromatic compounds but also hydrophobic substitutions such as piperidine moiety are very significant effect to display NTR based cancer terapy of any molecule. Hence, this information provides a useful insight for the development of novel prodrug(s) with specific selectivity.

According to enzymatic reduction analyses, in **A5**/Ssap-NtrB reaction, almost all of **A5** was converted to its metabolite retained ar 14 min, and upon 16 hours of incubation the stability of the metabolite was conserved. For **A17**/Ssap-NtrB reaction, 10 min and 200 µM NADH was not enough in order to continue the reduction reaction until the last step. Upon the reaction with the cofactor regeneration system, small amount of metabolites (around 6%) has started to be produced (Figure S59). As a similar case, the metabolite retained at 13.48 min remained stable after overnight incubation of **A20**/Ssap-NtrB reaction within the cofactor regeneration system.

As a result of biological studies, it was determined that, **A7, A10** and **A12-A14** compounds were toxic for Hepatoma and Prostate carcinoma cells and also HUVEC cells which was chosen as a healthy model. **A2, A9, A15** and **A23** were low toxic. Selected non-toxic compounds were searched for their prodrug ability. **A20/Ssap-NtrB, A5/Ssap-NtrB** and **A6/Ssap-NtrB** combinations were suggested to be potential prodrugs for prostate carcinoma cells according to *in vitro* analyses.

When we combine our theoretical, enzymatic and cytotoxic results, we foresee that **A5/Ssap-NtrB** combination can be a new promising prodrug candidate for NTR based cancer therapy.

4. EXPERIMENTAL SECTION

4.1. General Information

Analytical grade of all chemicals were purchased from Merck, Fluka and Sigma-Aldrich and were used as supplied without prior purification. 1,2-Diaminocyclohexane and 1,3-diaminocyclohexane were used at reactions as *cis*- and *trans*- mixture. NADH and NADPH were supplied from Roche Applied Science.

Melting points were measured with X-4 Melting-point Apparatus and were uncorrected. Organic synthesis were monitored by TLC on 0.25 mm silica gel plates (60GF254) and visualized with UV light and/or $KMnO_4$ stain. Infrared spectras were obtained by a Perkin Elmer Spectrum 100 FTIR spectrophotometer using ATR techniques. The ^{1}H-NMR and ^{13}C-NMR spectras were recorded on Varian Mercury 500 MHz, Agilent 600 MHz and Jeol 400 MHz NMR High-Performance Digital FT-NMR spectrometer, using TMS as an internal standard and using chloroform-d or DMSO-d6 as solvent. Splitting patterns are designated as follows: s, singlet; d, doublet; t, triplet; q, quadruplet; m, multiplet; dd, double doublet; dt, double triplet; td, triple doublet and ddd, double double doublet.

Ssap-NtrB recombinant enzyme was purified via Nickel HiTrap™ column (Amersham Biosciences) as stated in Celik and Yetis, 2012. Enzymatic activities were measured by using UV-VIS-NIR spectrophotometer (Shimadzu UV-3600) and microplate reader (Moleculer Devices Spectromax Plus 384). Metabolites of enzymatic reactions were determined with HPLC (Shimadzu High Performance Liquid Chromatography). CEM SP Discover Microwave Synthesis Reactor was used in microwave experiments by applying dynamic mode. Teledyne Isco Rf 200 CombiFlash Chromatagraphy was used to purify few crude products. Elemental analyses for C, H and N were obtained by Thermo, Flash 200 Organic Elemental Analyzer. Origin Pro 8.5 program was used for drawing all cytotoxicity and HPLC graphs. The measurements were performed in triplicate and error bars indicated ± standard deviations.

4.2. Synthesis of Prodrugs

***N*-(3,5-Dinitrophenyl)acetamide (A1).** 3,5-dinitroaniline (16.5 mmol; 3.0 g) was dissolved in 10 mL pyridine. Acetic anhydride (39.9 mmol; 3.75 mL; 2.4 equiv.) was added dropwise to the solution in an ice bath. Mixture was stirred at room temperature for 24h. After completion of the reaction, the mixture was poured into cold water (100 mL) and the solid was filtered and dried. The crude product was recrystallized from ethyl alcohol to give green

solid A1 [50] (3.5 g, 92% yield) mp 189 °C (lit. m.p. 191°C [51]); IR (ATR) ϑ 3274, 3112, 3097, 2944, 2871, 1683, 1604, 1542, 1420, 1340, 1328, 1267, 1252, 1078, 900, 818, 728 cm^{-1}; ^{1}H NMR (500 MHz, DMSO-d_6) δ10.80 (s, 1H), 8.78 (d, *J*= 2.08 Hz, 2H), 8.45 (t, *J*= 2.10 Hz, 1H), 2.12 (s, 3H); ^{13}C NMR (125 MHz, DMSO-d_6) δ 170.08, 148.62, 141.67, 118.53, 112.43, 24.54.

***N*-(3,5-Dinitrophenyl)-*N*-ethylacetamide (A2).** A solution of NaH (6.5 mmol; 0.155 g; 2.5 equiv; 55 % oil dispersion) in DMF (3 mL) was added to a solution of *N*-(3,5-dinitrophenyl)acetamide (A1) (6.6 mmol; 1.5 g) in DMF (10 mL) dropwise and stirred at room temperature for 1.5h. Then, ethyl iodide (19.8 mmol; 1.58 mL; 3 equiv.) was added to the reaction mixture and stirred at room temperature for 24h. After completion of the reaction, the mixture was poured into cold water and extracted with dichloromethane (30 mL × 3). The organic layer was washed with water (20 mL x 2) was dried over Na_2SO_4 and concentrated in vacuo. The oily residue was purified by column chromatography on silica gel (dichlorometane/methanol, 50:1) to provide yellow solid A2 [52]. (0.7g, 42% yield) mp 126-127 °C; IR (ATR) ϑ 3100, 3060, 2986, 2940, 2879, 1658, 1621, 1532, 1448, 1392, 1345, 1292, 1268, 1154, 1076, 911, 850, 731 cm^{-1}; ^{1}H NMR (500 MHz, DMSO-d_6) δ 8.75 (s, 1H), 8.61 (s, 2H), 3.79 (q, *J*= 6.78 Hz, 2H), 1.95 (s, 3H), 1.04 (t, *J*= 7.07 Hz, 3H); ^{13}C NMR (125 MHz, DMSO-d_6) δ 198.12, 148.93, 144.82, 129.29, 117.39, 42.54, 23.04, 13.53; LC/MS (ESI) *m/z*: 252.0 $[M - H]^-$.

***N*-(2-Bromo-5-nitrophenyl)acetamide (A3).** A3 was synthesized from 2-bromo-5-nitroaniline and acetic anhydride by using acetic acid and sulfuric acid at reflux conditions for 4h according to the procedure described in ref. 40. Yellow-green solid (81% yield) mp 182 °C (lit. m.p. 187 °C [40]); IR (ATR) ϑ 3290, 3104, 3025, 2971, 2936, 1663, 1608, 1537, 1456, 1350, 1328, 1298, 1033, 894, 826, 737 cm^{-1}; ^{1}H NMR (500 MHz, DMSO-d_6) δ 9.74 (s, 1H),

8.56 (d, *J*= 2.62Hz, 1H), 7.93 (m, 1H), 7.90 (m, 1H), 2.14 (s, 3H); ^{13}C NMR (125 MHz, DMSO-d_6) δ 169.93, 147.23, 137.96, 134.35, 120.95, 120.50, 23.89.

***N*-(2-Bromo-5-nitrophenyl)-*N*-ethylacetamide (A4).** A4 was obtained from A3 (3.86 mmol; 1.0 g; 2 equiv.) and ethyl iodide (11.6 mmol; 1.8 g; 0.92 mL; 3 equiv.) with NaH in 55 % oil dispersion (4.23 mmol; 0.185 g; 1.1 equiv.) by following the procedure described above for A2. After completion of the reaction, the mixture was poured into cold water (100 mL) and brown solid was obtained. The crude product was purified by column chromatography on silica gel ($CHCl_3$) to provide light yellow solid A4. (0.9 g, 82% yield) mp 128-129 °C; IR (ATR) ϑ 3100, 3061, 2990, 2940, 2877, 1652, 1569, 1521, 1471, 1396, 1346, 1300, 1249, 1036, 998, 863, 778, 739 cm^{-1}; ^{1}H NMR (400 MHz, DMSO-d_6) δ 8.33 (d, *J*= 2.66 Hz, 1H), 8.18 (td, *J*= 8.82 and 2.68 Hz, 1H), 8.13 (d, *J*= 8.81 Hz, 1H), 3.32 (q, *J*= 7.20 Hz, 2H), 1.70 (s, 3H), 1.04 (t, *J*= 7.21 Hz, 3H); ^{13}C NMR (100 MHz, DMSO-d_6) δ 168.75, 148.19, 142.44, 135,23, 132.06, 126.50, 125.00, 42.76, 22.84, 13.16; LC/MS (ESI) *m/z*: 289.0 $[M + H]^+$.

4-(4-Nitrobenzoyl)piperidine (A5). A mixture of piperidine (5.39 mmol; 0.46 g; 0.53 mL), 4-nitrobenzoyl chloride (5.39 mmol; 1.0 g) and potassium carbonate (8.08 mmol; 1.11 g; 1.5 equiv.) was stirred in 10 mL acetonitrile at reflux condition for 6h. Upon completion as shown by TLC, the mixture was poured into cold water (100 mL). The resulting solid was filtered, dried in room temperature and recrystallized with ethyl alcohol. (0,8 g, 63% yield) mp 115-118 °C (lit. m.p. 120 °C) [53]; IR (ATR) ϑ 3099, 3065, 3011, 2937, 2914, 2855, 1625, 1596, 1512, 1442, 1345, 1274, 1001, 849 cm^{-1}; ^{1}H NMR (400 MHz, DMSO-d_6) δ 8.23 (d, *J*= 8.74 Hz, 2H), 7.60 (d, *J*= 8.74 Hz, 2H), 3.56 (m, 2H), 3.16 (m, 2H), 1.55 (m, 4H), 1.40 (m, 2H); ^{13}C NMR (100 MHz, DMSO-d_6) δ 167.41, 148.13, 143.39, 128.44, 124.32, 48.38, 42.78, 26.35, 25.67, 24.43.

4-(4-Nitrobenzoyl)morpholine (A6). A mixture of morpholine (5.39 mmol; 0.47 g; 0.47 mL), 4-nitrobenzoyl chloride (5.39 mmol; 1.0 g) and triethylamine (8.08 mmol; 0.81 g; 1.11

mL; 1.5 equiv.) was stirred in 25 mL CH_2Cl_2 at reflux condition for 8h. Upon completion as shown by TLC, solvent was evoparated in vacuo to dryness. 15 mL ether was added to the residue and resulting cream solid was filtered, dried at room temperature. The crude solid was recrystallized with ethyl alcohol. (1.15 g, 90% yield) mp 102-103°C [54] ; IR (ATR) ϑ 3103, 3068, 2974, 2915, 2869, 1621, 1596, 1512, 1440, 1348, 1260, 1106, 1008, 836 cm^{-1}; ^{1}H NMR (400 MHz, DMSO-d_6) δ 8.25 (d, *J*= 8.79 Hz, 2H), 7.65 (d, *J*= 8.84 Hz, 2H), 3.615 (m, 4H), 3.50 (m, 2H), 3.23 (m, 2H); ^{13}C NMR (100 MHz, DMSO-d_6) δ 167.71, 148.33, 142.41, 128.91, 124.31, 66.44, 56.55.

General procedure for synthesis of A7-A14. 4-Dibutylamino-3,5-dinitrobenzoic acid, starting material for the synthesis A13 and A14 was obtained from 4-chloro-3,5-dinitrobenzoic acid and dibutylamine in methanol at reflux conditions for 3h according to the procedure described in ref. 55. Orange solid (84% yield) mp 140-141°C (lit. m.p. 139°C) [55]; IR (ATR) ϑ 3300-2243, 3074, 2960, 2934, 2874, 1690, 1609, 1530, 1421, 1349, 1095, 915, 761 cm^{-1}.

A solution of aniline derivatives (1.5 equiv.), dicyclohexylcarbodiimide (DCC) (1.3 equiv.) and 4-*N*,*N*-dimethylaminopyridine (DMAP) (0.3 equiv.) was added dropwise to a stirred solution of benzoic acid derivative (1 equiv.) in 20-40 mL of dichloromethane at room temperature. After completion of the addition the mixture was stirred at room temperature for 12-24h. Reaction mixture was diluted with water and extracted with ethyl acetate (3 x 50 mL). The combined organic layer was washed with water, dried with anhydrous Na_2SO_4, and concentrated in vacuo. The crude products were purified by washing eter, ethanol or ethyl acetate/ethyl alcohol to give A7-A14 [55].

3,5-Dinitro-*N*-(2,4-dinitrophenyl)benzamide (A7) . The reaction was performed under the same conditions as described above, using 3,5-dinitrobenzoic acid (5.0 mmol; 1.06 g), 2,4-dinitroaniline (7.5 mmol; 1.37 g; 1.5 equiv.), DCC (6.5 mmol; 1.34 g; 1.3 equiv.) and DMAP

(1.5 mmol; 0.18 g; 0.3 equiv.) with 24h reaction time. The crude product was purified by Combi Flash chromatagraphy technique (silicagel, hexane:ethyl acetate 1:1, 60 min) to give A7. (0.5 g, 38% yield) mp 192-194 °C (lit. m.p. 213°C) [56]; IR (ATR) ϑ 3323, 3103, 1675, 1624, 1607, 1534, 1339, 1311, 1242, 1079, 914, 835, 730 cm^{-1}; ^{1}H NMR (400 MHz, DMSO-d_6) δ ^{1}H NMR (400 MHz, DMSO-d_6) δ 11.71 (s, broad, 1H), 9.08 (d, *J*= 2.08 Hz, 2H), 9.01 (t, *J*= 2.00 Hz, 1H), 8.72 (t, *J*= 2.68 Hz, 1H), 8.59 (dd, *J*= 8.94 and 2.63 Hz, 1H), 7.935 (dd, *J*= 8.9 and 3.63 Hz, 1H); ^{13}C NMR (100 MHz, DMSO-d_6) δ 162.47, 148.86, 144.33, 142.84, 136.47, 135.84, 129.09, 128.66, 127.52, 122.63, 121.73; LC/MS (ESI) *m/z*: 376.0 $[M - H]^-$.

4-Methyl-3,5-dinitro-*N*-(4-nitrophenyl)benzamide (A8). The reaction was performed under the same conditions as described above, using 4-methyl-3,5-dinitrobenzoic acid (1.0 mmol; 0.23 g), 4-nitroaniline (1.5 mmol; 0.21 g; 1.5 equiv.), DCC (1.3 mmol; 0.27 g; 1.3 equiv.) and DMAP (0.3 mmol; 0.04 g; 0.3 equiv.) with 24h reaction time. The crude product was purified by washing with ethyl acetate/ethanol to give A8. (0.07 g, 20% yield) mp 246-247 °C; IR (ATR) ϑ 3410, 3084, 2931, 1683, 1595, 1538, 1495, 1407, 1329, 1262, 1229, 1113, 9001, 852, 744, 722 cm^{-1}; ^{1}H NMR (500 MHz, DMSO-d_6) δ 11.09 (s, 1H), 8.78 (s, 2H), 8.27 (d, *J*= 8.83 Hz, 2H), 8.05 (d, *J*= 9.27 Hz, 2H), 2.53 (s, 3H); ^{13}C NMR (125 MHz, DMSO-d_6) δ 162.46, 151.29, 144.97, 143.44, 134.15, 130.44, 127.42, 125.27, 120.64, 15.23; LC/MS (ESI) *m/z*: 345.0 $[M - H]^-$.

4-Methyl-3,5-dinitro-*N*-(2,4-dinitrophenyl)benzamide (A9). The reaction was performed under the same conditions as described above, using 4-methyl-3,5-dinitrobenzoic acid (5.0 mmol; 1.3 g), 2,4-dinitroaniline (7.5 mmol; 1.37 g; 1.5 equiv.), DCC (6.5 mmol; 1.34 g; 1.3 equiv.) and DMAP (1.5 mmol; 0.18 g; 0.3 equiv.) with 24h reaction time. The crude product was purified by washing with ethanol to give grey solid A9. (0.27 g, 48% yield) mp 180-184 °C; IR (ATR) ϑ 3324, 3083, 1702, 1686, 1601, 1497, 1331, 1259, 1141, 908, 835, 739 cm^{-1}; ^{1}H NMR (400 MHz, DMSO-d_6) δ 11.53 (s, broad, 1H), 8.73 (s, 2H), 8.695 (d,

J= 2.6 Hz, 1H), 8.55 (dd, *J*= 8.99 and 2.63 Hz, 1H), 7.93 (d, *J*= 8.99 Hz, 1H), 2.52 (s, 3H). ^{13}C NMR (100 MHz, DMSO-d_6) δ 162.57, 151.55, 143.94, 142.66, 137.18, 133.17, 131.26, 129.01, 127.54, 127.20, 121.68, 15.44; LC/MS (ESI) *m/z*: 390.0 $[M - H]^-$.

***N*-(4-Chlorophenyl)-4-(dimethylamino)-3,5-dinitrobenzamide (A10).** The reaction was performed under the same conditions as described above, using 4-(dimethylamino)-3,5-dinitrobenzoic acid (1.0 mmol; 0.26 g), 4-chloroaniline (1.5 mmol; 0.2 g; 1.5 equiv.), DCC (1.3 mmol; 0.27 g; 1.3 equiv.) and DMAP (0.3 mmol; 0.04 g; 0.3 equiv.) with 24h reaction time. The crude product was purified by washing with ethanol to give orange solid A10. (0.27 g, 74% yield) mp 170-174 °C; IR (ATR) ϑ 3240, 3323, 3070, 3034, 2928, 1672, 1619, 1528, 1350, 1309, 1242, 1186, 1088, 962, 892, 827, 743, 641 cm^{-1}; ^{1}H NMR (500 MHz, DMSO-d_6) δ 10.54 (s, 1H), 8.64 (s, 2H), 7.77 (dt, *J*= 8.87 and 3.1 Hz, 2H), 7.43 (dt, *J*= 8.86 and 3.1 Hz, 2H), 2.82 (s, 6H); ^{13}C NMR (125 MHz, DMSO-d_6) δ 161.95, 143.25, 140.91, 138.03, 129.96, 129.09, 128.17, 124.79, 122.37, 42.39; LC/MS (ESI) *m/z*: 363.0 $[M - H]^-$.

4-(Dimethylamino)-3,5-dinitro-*N*-(4-nitrophenyl)benzamide (A11). The reaction was performed under the same conditions as described above, using 4-(dimethylamino)-3,5-dinitrobenzoic acid (1.0 mmol; 0.26 g), 4-nitroaniline (1.5 mmol; 0.21 g; 1.5 equiv.), DCC (1.3 mmol; 0.27 g; 1.3 equiv.) and DMAP (0.3 mmol; 0.04 g; 0.3 equiv.) with 24h reaction time. The crude product was purified by washing with ethyl acetate/ethanol to give orange solid A11. (0.2 g, 53% yield) mp 266-268 °C; IR (ATR) ϑ 3422, 3137, 3073, 2889, 1684, 1613, 1528, 1498, 1404, 1329, 1298, 1238, 1181, 1100, 1069, 851, 749, 711 cm^{-1}; ^{1}H NMR (500 MHz, DMSO-d_6) δ 10.88 (s, 1H), 8.64 (s, 2H), 8.255 (d, *J*= 8.96 Hz, 2H), 7.99 (d, *J*= 9.01 Hz, 2H), 2.81 (s, 6H); ^{13}C NMR (125 MHz, DMSO-d_6) δ 162.58, 145.33, 143.17, 143.05, 141.13, 130.29, 125.26, 124.01, 120.43, 42.42; LC/MS (ESI) *m/z*: 374.0 $[M - H]^-$.

4-(Dimethylamino)-3,5-dinitro-*N*-(2,4-dinitrophenyl)benzamide (A12). The reaction was performed under the same conditions as described above, using 4-(dimethylamino)-3,5-

dinitrobenzoic acid (1.0 mmol; 0.26 g), 2,4-dinitroaniline (1.5 mmol; 0.27 g; 1.5 equiv.), DCC (1.3 mmol; 0.27 g; 1.3 equiv.) and DMAP (0.3 mmol; 0.04 g; 0.3 equiv.) with 24h reaction time. The crude product was purified by washing with ethyl acetate/ethanol to give orange solid A12. (0.21 g, 50% yield) mp 197-199 °C; IR (ATR) ϑ 3345, 3117, 3062, 2929, 1703, 1602, 1536, 1496, 1456, 1334, 1241, 1131, 946, 910, 853, 740 cm^{-1}; ^{1}H NMR (500 MHz, DMSO-d_6) δ 11.32 (s, 1H), 8.72 (dd, *J*= 2.61 and 0.88 Hz, 1H), 8.61 (d, *J*= 0.97 Hz, 2H), 8.58 (ddd, *J*= 8.46, 2.66 and 1.04 Hz, 1H), 7.93 (dd, *J*= 8.92 and 0.63 Hz, 1H), 2.84 (s, 6H); ^{13}C NMR (125 MHz, DMSO-d_6) δ 162.38, 143.81, 143.02, 142.23, 141.62, 136.82, 130.42, 128.97, 126.80, 122.27, 121.64, 42.52; LC/MS (ESI) *m/z*: 419.0 $[M - H]^-$.

***N*-(4-Chlorophenyl)-4-(dibutylamino)-3,5-dinitrobenzamide (A13).** The reaction was performed under the same conditions as described above, using 4-(dibutylamino)-3,5-dinitrobenzoic acid (2.95 mmol; 1.00 g), 4-chloroaniline (4.42 mmol; 0.56 g; 1.5 equiv.), DCC (3.83 mmol; 0.79 g; 1.3 equiv.) and DMAP (0.88 mmol; 0.11 g; 0.3 equiv.) with 12h reaction time. The crude product was purified by washing with ether and ethanol to give yellow solid A13. (1.05 g, 79% yield) mp 149-152°C; IR (ATR) ϑ 3425, 3323, 2959, 2928, 2851, 1670, 1613, 1525, 1397, 1347, 1311, 1242, 1088, 919, 831, 743 cm^{-1}; ^{1}H NMR (400 MHz, DMSO-d_6) δ 10.51 (s, 1H), 8.55 (s, 2H), 7.71 (d, *J*= 8.93 Hz, 2H), 7.38 (d, *J*= 8.92 Hz, 2H), 2.93 (t, *J*= 7.32 Hz, 4H), 1.41 (m, 4H), 1.17 (m, 4H), 0.76 (t, *J*= 7.35 Hz, 6H); ^{13}C NMR (100 MHz, DMSO-d_6) δ 162.10, 157.11, 145,65, 139.93, 138.08, 129.42, 129.20, 128.30, 122.43, 52.01, 29.81, 19.77, 14.10; LC/MS (ESI) *m/z*: 447.0 $[M - H]^-$.

***N*-(4-Nitrophenyl)-4-(dibutylamino)-3,5-dinitrobenzamide (A14).** The reaction was performed under the same conditions as described above, using 4-(dibutylamino)-3,5-dinitrobenzoic acid (2.95 mmol; 1.00 g), 4-nitroaniline (4.42 mmol; 0.61 g; 1.5 equiv.), DCC (3.83 mmol; 0.79 g; 1.3 equiv.) and DMAP (0.88 mmol; 0.11 g; 0.3 equiv.) with 12h reaction time. The crude product was purified by washing with ether and ethanol to give yellow solid

A14. (0.9 g, 67% yield) mp 165-167 °C; IR (ATR) ϑ 3424, 3324, 2928, 2850, 1681, 1615, 1533, 1490, 1306, 1241, 1087, 892, 739 cm^{-1}; ^{1}H NMR (400 MHz, DMSO-d_6) δ 10.89 (s, 1H), 8.58 (s, 2H), 8.235 (d, *J*= 9.23 Hz, 2H), 7.955 (d, *J*= 9.24 Hz, 2H), 2.94 (t, *J*= 7.30 Hz, 4H), 1.42 (m, 4H), 1.18 (m, 4H), 0.76 (t, *J*= 7.35 Hz, 6H); ^{13}C NMR (100 MHz, DMSO-d_6) δ 162.74, 157.11, 145.21, 143.31, 140.23, 129.79, 126.35, 125.37, 120.52, 51.98, 29.76, 19.77, 14.09; LC/MS (ESI) *m/z*: 458.0 $[M - H]^-$.

General procedure for synthesis of A15-A17. A solution of 4-nitrobenzoyl chloride (2 equiv.) in DMF (10 mL) was cooled with an ice bath, then the corresponding reactant (ethylenediamine, 1,4-diaminobutane or piperazine) (1 equiv.) and triethylamine (2.1 equiv.) was added dropwise. The reaction was performed at 50 °C for 6h. Upon completion as shown by TLC, the mixture was poured into cold water (100 mL). The resulting solid was filtered and dried at room temperature.

***N,N'*-(Ethane-1,2-diyl)bis(4-nitrobenzamide) (A15).** The reaction was performed under the same conditions as described above, using 4-nitrobenzoyl chloride (6.66 mmol; 1.24 g; 2 equiv.) and ethylenediamine (3.33 mmol; 0.2 g; 0.22 mL; 1 equiv.) with triethylamine (7.0 mmol; 0.7 g; 0.96 mL; 2.1 equiv.). The crude product was purified by washing with hot acetone to give white solid A15. (0.6 g, 50% yield) mp 259-261 °C (dec.) (lit. m.p. 255-257 °C) [57]. IR (ATR) ϑ 3313, 3113, 3093, 3076, 3056, 2939, 2856, 1637, 1597, 1543, 1517, 1487, 1444, 1331, 1106, 1011, 847 cm^{-1}; ^{1}H NMR (400 MHz, DMSO-d_6) δ 8.89 (m, 2H), 8,.26 (m, 4H), 8.01 (m, 4H), 3.41 (m, 4H); ^{13}C NMR (100 MHz, DMSO-d_6) δ 165.44, 149.49, 140.72, 129.24, 124.05, 40.01.

***N,N'*-(Butane-1,4-diyl)bis(4-nitrobenzamide) (A16)** [58] The reaction was performed under the same conditions as described above, using 4-nitrobenzoyl chloride (6.80 mmol; 1.26 g; 2 equiv.) and 1,4-diaminobutane (3.40 mmol; 0.3 g; 0.34 mL; 1 equiv.) with triethylamine (7.48 mmol; 0.75 g; 1.03 mL; 2.2 equiv.). The crude product was purified by washing with

hot acetone and hot CH_2Cl_2 to give white solid A16. (0.81g, 62% yield) mp 268-269°C; IR (ATR) ϑ 3334, 3109, 3074, 3046, 2977, 2954, 2868, 1633, 1588, 1538, 1520, 1488, 1446, 1348, 1118, 1016, 866 cm^{-1}; ^1H NMR (400 MHz, DMSO-d_6) δ8.78 (t, *J*= 5.52 Hz, 2H), 8.265 (d, *J*= 8.91 Hz, 4H), 8.015 (d, *J*= 8.94 Hz, 4H), 3.28-3.27 (m, *J*= 9.24 Hz, 4H), 1.55 (m, 4H); ^{13}C NMR (100 MHz, DMSO-d_6) δ 164.99, 149.42, 140.74, 129.16, 124.04, 40.60, 26.97; Anal. Calcd for $C_{18}H_{18}N_4O_6$: C, 55.96; H, 4.70; N, 14.50. Found: C, 55.39; H, 4.65; N, 14.03.

1,4-Bis(4-nitrobenzoyl)piperazine (A17). The reaction was performed under the similar conditions as described above, using 4-nitrobenzoyl chloride (6.96 mmol; 1.29 g; 2 equiv.) and piperazine (3.48 mmol; 0.3 g; 1 equiv.) with triethylamine (7.66 mmol; 0.77 g; 1.06 mL; 2.2 equiv.) at room temperature for 5h. The crude product was purified by washing with hot acetone to give white solid A17. (0.74 g, 55% yield) mp >300 °C (lit. m.p. 318 °C) [59]; IR (ATR) ϑ 3103, 3068, 3040, 3001, 2926, 2869, 1620, 1587, 1513, 1437, 1349, 1266, 1001, 847 cm^{-1}; ^1H NMR (400 MHz, DMSO-d_6) δ 8.26 (m, 4H), 7.67 (m, 4H), 3.80-3.20 (m, 8H); ^{13}C NMR (100 MHz, DMSO-d_6) δ 167.81, 148.35, 142.31, 128.83, 124.23, 48.61.

General procedure for synthesis of cyclohexyl containing benzamide derivatives (A18-A20). 4-Nitrobenzoyl chloride (5.38 mmol; 1.0 g; 2.0 equiv.) was dissolved in 20 mL chloroform. Triethylamine (6.46 mmol; 0.65 g; 0.9 mL; 2.4 equiv.) and diaminocyclohexane derivatives (1,2-diaminocyclohexane, 1,3-diaminocyclohexane, 1,4-diaminocyclohexane) (2.69 mmol; 0.31 g) were added to the reaction mixture, respectively. After completion of the addition, the solution was refluxed at variable reaction times (8-14h). After completion of the reaction detected by TLC, the resulting solid was filtered and washed with water (50 mL) and then dried at room temperature [60].

***N,N'*-(1,2-Cyclohexyl)bis(4-nitrobenzamide) (A18).** The reaction was performed under the same conditions as described above, using *cis,trans*-1,2-diaminocyclohexane with 14 h reaction time. The crude product was purified by washing with hot methanol to give white

795 solid A18 [61]. (0.78 g, 70% yield) mp >300 °C (lit. m.p. 338 °C); IR (ATR) ϑ 3274, 3088,
796 2957, 2946, 2933, 2862, 1640, 1600, 1583, 1516, 1454, 1383, 1344, 1146, 1011, 867 cm^{-1}; ^{1}H
797 NMR (400 MHz, DMSO-d_6) δ 8.635 (d, *J*= 8.19 Hz, 2H), 8.205 (d, *J*= 8.82 Hz, 4H), 7.86 (d,
798 *J*= 8.82 Hz, 4H), 3.95-3.91 (m, 2H), 1.85-1.23 (m, 8H); ^{13}C NMR (100 MHz, DMSO-d_6) δ
799 165.15, 149.28, 141.11, 129.09, 124.00, 123.85, 53.55, 31.86, 25.18.

800 ***N,N'*-(1,3-Cyclohexyl)bis(4-nitrobenzamide) (A19).** The reaction was performed under
801 the same conditions as described above, using c*is,trans*-1,3-diaminocyclohexane with 8h
802 reaction time to give white solid A19. (0.72 g, 65% yield) mp >300 °C (lit. m.p. 329-330 °C)
803 [62]; IR (ATR) ϑ 3264, 3109, 3078, 2942, 2857, 1637, 1600, 1543, 1514, 1448, 1341, 1151,
804 1014, 867 cm^{-1}; ^{1}H NMR (400 MHz, DMSO-d_6) **(*cis*-, *trans*- mixture)** δ 8.64 (d, *J*= 7.84 Hz,
805 2H), 8.54 (d, *J*= 7.37 Hz, 2H), 8.26 (d, *J*= 8.81 Hz, 4H and d, *J*= 8.81 Hz, 4H), 8.03 (d, *J*=
806 8.77 Hz, 4H and d, *J*= 8.77 Hz, 4H), 4.26 (m, 2H), 3.865 (m, 2H), 2.07-2.04 (m, 4H), 1.86-
807 1.76 (m, 4H), 1.68 (m, 4H), 1.45-1.24 (m, 4H); ^{13}C NMR (100 MHz, DMSO-d_6) **(*cis*-, *trans*-**
808 **mixture)** δ 165.00, 164.29, 149.40, 149.35, 141.13, 140.89, 129.53, 129.33, 123.96, 123.88,
809 48.33, 48.21, 47.85, 45.57, 45.51, 45.39, 38.87, 35.94, 34.63, 31.72, 30.98, 29.52, 23.45,
810 21.51, 20.11.

811 ***N,N'*-(1,4-Cyclohexyl)bis(4-nitrobenzamide) (A20).** The reaction was performed under
812 the same conditions as described above, using *trans*-1,4-diaminocyclohexane with 9h reaction
813 time. The crude product was purified by washing with hot acetone to give white solid A20.
814 (0.83 g, 75% yield) mp >300 °C; IR (ATR) ϑ 3293, 3109, 3070, 2946, 2867, 1633, 1600,
815 1537, 1516), 1458, 1344, 1107, 1014, 869 cm^{-1}; ^{1}H NMR (400 MHz, DMSO-d_6) δ 8.59 (d,
816 *J*=7.79 Hz, 2H), 8.27 (d, *J*=8.90 Hz, 4H), 8.03 (d, *J*=8.91 Hz, 4H), 3.76 (m, 2H), 1.93-1.89
817 and 1.47-1.29 (m, 8H); ^{13}C NMR (100 MHz, DMSO-d_6) δ 164.35, 149.36, 140.82, 12923,
818 123.86, 48.47, 28.65; LC/MS (ESI) *m/z*: 411.0 $[M - H]^-$.

General procedure for synthesis of phenylene containing benzamide derivatives (A21-A23). Diaminobenzene derivatives (1,2-diaminobenzene, 1,3-diaminobenzene, 1,4-diaminobenzene) (2.77 mmol; 0.3g) was dissolved in 5 mL pyridine at a 35 mL microwave reaction vessel. 4-Nitrobenzoyl chloride (5.82 mmol; 1.08 g; 2.1 equiv.) and DMAP (0.138 mmol; 17 mg; 0.05 equiv.) were added and stirred at room temperature for 5 min to obtain a homogeneous reaction medium. The mixture was heated at 70°C under microwave irradiation for 20-25 min. After completion of the reaction detected by TLC, the mixture was warmed to room temperature. 25 mL ice-water was added and the resulting solid was filtered. Then the crude product was washed with diluted HCl solution (40 mL x 2), water (50 mL), diluted NaOH solution (50 mL) and again water (50 mL), respectively and dried at room temperature [63].

***N,N'*-(1,2-Phenylene)bis(4-nitrobenzamide) (A21).** The reaction was performed under the same conditions as described above, using 1,2-diaminobenzene with 20 min reaction time. The crude product was purified by washing with hot acetone and hot toluene to give yellow solid A21 (0.56 g, 50% yield) mp >300 °C (lit. m.p. 300 °C) [64]; IR (ATR) ϑ 3274, 3136, 3114, 3058, 1659, 1597, 1529, 1509, 1343, 1108, 1012, 862, 766 cm^{-1}; ^{1}H NMR (400 MHz, DMSO-d_6) δ 10.27 (s, 2H), 8.32 (d, *J*= 9.09 Hz, 4H), 8.13 (d, *J*= 9.12 Hz, 4H), 7.63 (t, *J*= 5.10 Hz, 2H), 7.29 (t, *J*= 4.97 Hz, 2H); ^{13}C NMR (100 MHz, DMSO-d_6) δ 164.54, 149.68, 140.75, 131.76, 129.74, 126.79, 126.46, 124.16.

***N,N'*-(1,3-Phenylene)bis(4-nitrobenzamide) (A22).** The reaction was performed under the same conditions as described above, using 1,3-diaminobenzene with 25 min reaction time. The crude product was purified by washing with hot acetone and hot hexane/cyclohexane to give green solid A22 (0.73 g, 65% yield) mp 269-271 °C (lit. m.p. 271 °C) [65]; IR (ATR) ϑ 3330, 3110, 3082, 3053, 3037, 1645, 1603, 1537, 1323, 1116, 1014, 868, 842 cm^{-1}; ^{1}H NMR (600 MHz, DMSO-d_6) δ 10.63 (s, 2H), 8.36 (d, *J*=8.53 Hz, 5H), 8.185 (d, *J*=8.59 Hz, 4H),

7.525 (d, *J*=8.11 Hz, 2H), 7.36 (t, *J*=8.09 Hz, 1H); ^{13}C NMR (150 MHz, DMSO-d_6) δ 164.39, 149.61, 141.03, 139.44, 129.70, 129.28, 123.96, 116.93, 113.32.

***N,N'*-(1,4-Phenylene)bis(4-nitrobenzamide) (A23).** The reaction was performed under the same conditions as described above, using 1,4-diaminobenzene with 20 min reaction time. The crude product was purified by washing with hot chloroform and hot acetone to give grey solid A23 (0.79 g, 71% yield) mp >300 °C (lit. m.p. 350 °C) [65]; IR (ATR) ϑ 3311, 3151, 3109, 3086, 3049, 1650, 1606, 1542, 1515, 1345, 1104, 1015, 870, 856, 823 cm^{-1}; ^{1}H NMR (600 MHz, DMSO-d_6) δ 10.57 (s, 2H), 8.34 (d, *J*= 8.77 Hz, 4H), 8.15 (d, *J*= 8.83 Hz, 4H), 7.74 (s, 4H); ^{13}C NMR (150 MHz, DMSO-d_6) δ 164.17, 149.58, 141.04, 135.33, 129.61, 123.99, 121.29.

4.3. Theoretical Calculations

4.3.1. ADMET studies

The entitled compounds were filtered using Lipinski [41] and Veber [42] rules to define drug-like compounds. Then, computer aided ADMET were used to help identify their pharmacokinetic properties and to select a lead candidate for further development. In this way, we can easily predict biological activities of the new chemical structures (ligands) and define the relationship between ligands and target based on experimental and clinical results.

ADMET studies; were employed using DS 2017 program of BIOVIA molecular modeling package [43]. These applications are only based on the chemical structure of the molecules. Firstly, the structures were (Figure 2) drawn and the descriptors were calculated. These are Aqueous solubility, Blood brain barrier penetration, Cytochrome P450 2D6 binding (CYP2D6), Hepatotoxicity, Intestinal absorption, Plasma protein binding and toxicities of the compounds using DS 2017.

4.3.2. Molecular Docking

This method to estimate small molecule, ligand-active sites in the enzyme was generated using ligand–enzyme molecular docking calculations with different approaches. The study involve five compounds which have three different analog frameworks and chosen based on the biological activity studies and ADMET analysis (Table 2).

4.3.3. Ligand structures optimization

All calculations were performed using Gaussian09 [66] and Discovery Studio softwares [43]. Each compound was minimized using DFT at the B3LYP hybrid functional and 6-31G* basis set in G09. The lowest energy conformations for all compounds were also determined by using conformational analysis technique in DS 2017.

4.3.4. Enzyme structure optimization

In our previous study [18, 39], the enzyme was modelled, optimized with applying homology modeling subprotocol and protein preparation tool in DS 2017 for molecular docking. CHARMm [67] based molecular dynamics (MD) was implemented to dock ligands into the enzyme active site.

Finally, ligand(s) and enzyme were interacted with default settings for all docking processes. Binding site was defined by using the related tool in DS 2017 and/or knowledge from literature. Based on i) Interaction types including hydrogen bond and non-bond interactions, ii) Energy and iii) TPSA and AlogP values of ligand in active site of the target protein were used to define selection of the compound in the studied compounds (Figure 7 and Table 3).

4.4. *S. Saprophyticus* nitroreductase assay

Recombinant Ssap-NtrB was expressed and purified as stated previously [18]. Ssap-NtrB activity against test compounds was assessed with the following protocol: Stock solutions of compounds were added to Tris/Cl buffer (25 mM, pH 7.5) in 5 % DMSO at 21-25 ^{o}C. **A5-A6** and **A15-23** compounds were able to dissolve in 15 % DMSO due to the solubility limits.

Upon the enzyme (2,5-30 µg/mL Ssap-NtrB) addition, the reaction was initiated by adding NADH (200-700 µM). Specific reaction conditions for each compound are given below:

A1, A2: 150 µM substrate was added to Tris/Cl buffer (25 mM, pH 7.5) in 5% DMSO including 30 µg/mL Ssap-NtrB and 636 µM NADH. The reaction mixture was incubated at 21 ^{o}C. **A3, A4, A8, A11, A12:** 100 µM substrate was added to Tris/Cl buffer (25 mM, pH 7.5) in 5% DMSO including 37 µg/mL Ssap-NtrB and 429 µM NADH. The reaction mixture was incubated at 21 ^{o}C. **A7, A9, A10, A13, A14:** 111 µM substrate was added to Tris/Cl buffer (25 mM, pH 7.5) in 5% DMSO including 44 µg/mL Ssap-NtrB and 444 µM NADH. The reaction mixture was incubated at 21 ^{o}C. **A5-A6** and **A15-A23:** 100 µM substrate was added to Tris/Cl buffer (25 mM, pH 7.5) in 15% DMSO including 30 µg/mLSsap-NtrB and 100 µM NADH in cofactor regeneration system (30 ug/mL CmFDH, 200 µM sodium formate and 10 µM NAD^{+}. The reaction mixture was incubated at 25 ^{o}C. **A5, A6:** 100 µM substrate was added to Tris/Cl buffer (25 mM, pH 7.5) in 10% DMSO including 2.5 µg/mL Ssap-NtrB and 200 µM NADH. The reaction mixture was incubated at 25 ^{o}C.

Aliquots from control and reaction samples were collected, the reaction was stopped with 1:1 cold acetonitrile and analyzed by RP-HPLC (RPC18 column:250 mm x 4.6 mm, 5 µm, UK) with acetonitrile (ACN) as the mobile phase. Analyses were performed with a flow rate of 1 mL/min and a gradient of 20-80% ACN (two HPLC programs were used; I: 0-5 min at 20% ACN, 15-22 min at 80% ACN, 27-32 min at 20% ACN. II: 0-5 min at 20% ACN, 25-35 min at 80% ACN, 40-45 min at 20% ACN).

The peak areas under HPLC chromatogram at 254 nm and 340 nm were used to determine the reduction of the starting compound as well as the appearance of reaction products.

Time dependent product profiles were assessed by coupled enzyme system (Ssap-NtrB/CmFDH) in order to allow cofactor regeneration. 100 µM prodrugs were dissolved in pH 7.5 Tris/Cl buffer with 5-15% DMSO. 100 µM NADH, 10 µM NAD+, 0.1 mg/mL BSA,

200 µM sodium formate, 30 µg/mL Ssap-NtrB and 30 µg/mL FDH were included in the reaction mixture and the reaction was incubated at 25 ^{o}C. 50 µL aliquots were taken with different time intervals and the reaction was stopped with 1:1 cold acetonitrile. HPLC analysis were performed at 254 nm and 340 nm as a function of time.

Michaelis–Menten kinetic parameters of Ssap-NtrB with prodrugs **A1** and **A2** were determined spectrophotometrically at 25 ºC in 25 mM Tris-CI buffer (pH 7.5) containing 5% DMSO as cosolvent. In a typical reaction, 0.4-31 µg/mL Ssap-NtrB was reacted with 0-800 µM substrate in the presence of 200 µM NADPH. Reactions were followed by the initial decrease in the amount of cofactor at 340 nm (NAD(P)H Ɛ340= 6220 M^{-1} cm^{-1}). One unit was defined as 1 µmol of NADPH catalyzed by Ssap-NtrB per minute.

4.5. Cytotoxic Assays

4.5.1. Cell culture and growth inhibitory effect of amides

Hep3B (Human Hepatoma carcinoma Cell line), PC3 (Human Prostate Carcinoma Cell line) and HUVEC (Human Umbilical Vein Cell line) cells were a kind gift from Cardiff University (Dr. Dipak Ramji), Ege University (Dr. İsmet GÜNERHAN) and Bilkent University (Dr. Ayşe Begüm Tekinay), respectively. Hep3B and HUVEC cells were cultured in High Glucose medium (High Clone) supplemented with 10% heat-inactivated (sterilized) fetal bovine serum (FBS;High Clone) and glutamine (2 mM-Sigma). For PC3 cells, low glucose medium (High Clone) was used. Cells were incubated in conditions of 37°C and 5% CO_2. To assess the cytotoxicity of the compounds against Hep3B and HUVEC cell lines, the cells were seed in 96 well plates ($5x10^4$ cells/well). After 24 h of attachment, the cells were treated with compounds at five different concentrations (150, 75, 39, 19 and 9 µM). DMSO was used as a vehicle control at final concentration of 1 %. After 48 h of exposure, MTT assay was performed as described in ref 49. The results were obtained using

spectrophotometer at 550 nm wavelength. % Cell viability value was calculated using this formula: (OD 550 sample/OD 550 control)*100.

4.5.2. Extracelluler Ssap-NtrB studies (Prodrug abilities of amides)

After MTT analyses, non-toxic compounds were referred to prodrug for using in reaction with *Staphylococcus saprophyticus* Nitroreductase (Ssap-NtrB). Previously, Ssap-NtrB was expressed and purified from *E. coli* strain by Gebze Technical University research group. The prodrug abilities of amides were determined using SRB assay against PC3 cells. The log-phase cells were seeded in 96-well plates in 200 µL DMEM containing 10% FBS (10.000 cells/well). After 24h incubation, cells were exposed to prodrug alone and to the mixture of prodrugs (150, 39 and 9 µM or 180, 18 and 1.8 nM) with cofactor (final concentration: 600 µM) and enzyme (final concentration 31 µg/mL) for 48h in 96-well plates under aerobic conditions. For CB1954 the quantity of NADH and Ssap/NtrB was 900 µM and 31 µg/mL, respectively. Cell survival was measured using the SRB assay [68]. Briefly, cells were plated in a 96-well plate, fixed in trichloroacetic acid (TCA) at final concentration of 12.5% for 1h at 4°C and washed with dH_2O then air-dried. Fixed cells were then stained with 0.4% sulforhodamine B in dH_2O for 30 min at room temperature, washed four times in 1% glacial acetic acid, and air dried. Bound sulforhodamine B was then solubilized in 100 µL of 10 mM Tris HCl pH 7.5. The extinction at 492 nm was read using thermo spectrophotometer, and results were expressed as a percentage of cell growth (cell survival). The IC_{50}s were evaluated by Origin pro 8.5. CB1954 was used as a positive control of Ssap-NtrB activity.

SUPPORTING INFORMATION

Supplementary data to this article can be found online at …… These document include spectroscopic datas of prodrugs, molecular docking outputs, detail enzymatic and cytotoxicity results.

ACKNOWLEDGMENTS

This study was financially supported by a research grant from Scientific and Technological Research Council of Turkey-TUBITAK (Grant No. 110T754 and 113Z706). Sincere thanks to Gizem TATAR for her supports to help computational part of this study. The numerical calculations reported in this abstract were fully performed at TUBITAK ULAKBIM, High Performance and Grid Computing Center (TRUBA resources).

ABBREVIATIONS

^{1}H NMR, proton nuclear magnetic resonance; GDEPT, Gene-directed enzyme prodrug therapy; NTR, nitroreductase; CB1954, 5-aziridinyl-2,4-dinitrobenzamide; SN 23862, 5-[*N*,*N*-bis(2-chloroethyl)amino]-2-hydroxyamino-4-nitrobenzamide; DNBM, dinitrobenzamide mustards; FT-IR, Fourier-transform infrared spectroscopy, ^{1}H NMR, Proton nuclear magnetic resonance; ^{13}C NMR, carbon nuclear magnetic resonance; MS, Mass spectroscopy; TLC, Thin-layer chromatography; UV, Ultraviolet; ATR, Attenuated Total Reflection; TMS, Tetramethylsilane; DMSO, dimethyl sulfoxide; SAR, Structure−activity relationship; Hep3B, Human Hepatoma Cell line); PC3, Human Prostate Carcinoma Cells; HUVEC, Human Umbilical Vein Cells; MTT, (3-(4,5-Dimethylthiazol-2-yl)-2,5-Diphenyltetrazolium Bromide); OD, Optical density; SRB, Sulforhodamine B (SRB) Assay; IC_{50} , 50 % inhibition concentration; ADMET, absorption, distribution, metabolism, and excretion - toxicity in pharmacokinetics; Comp, compound; ALogP, octanol/water partition coefficient, a measure for lipophilicity; MW, molecular weight; MPSA, molecular polar surface area; HA_Lipinski,

Number of hydrogen bond acceptors; HD_Lipinski, Num_H_Donors_Lipinski; Number of hydrogen bond donors; NRB, Number of Rotatable bonds; HA_Veber, Number of hydrogen bond acceptors based on Veber; HD_Veber, Number of hydrogen bond donors based on Veber; PSA, polar surface area; AlogP98, the logarithm of the partition coefficient between n-octanol and water; HIA, Human Intestinal Absorption, BBB blood brain barrier; CYP2D6 cytochrome P450 2D6 binding, PPB plasma protein binding, ΔG, Binding Energy; Ki, inhibition constant; TPSA, Topological polar surface area; CHARMm, Chemistry at HARvard Macromolecular Mechanics; MD, molecular Dynamics; G09, Gaussian 09; DS, Discovery Studio.

REFERENCES

[1] S. Bhaumik, T.V. Sekar, J. Depuy, J. Klimash, R. Paulmurugan, Noninvasive optical imaging of nitroreductase gene-directed enzyme prodrug therapy system in living animals. Gene Ther. 19 (2012) 295–302.

[2] W.A. Denny, Nitroreductase-based GDEPT. Curr. Pharm. Des., 8 (2002) 1349–1361.

[3] G. U. Dachs, J. Tupper, G.M. Tozer, From bench to bedside for gene-directed enzyme prodrug therapy of cancer. Anticancer Drugs, 16 (2005) 349-359.

[4] X. Zhang, X.Q. You, X. Zhang, Prodrug strategy for cancer cell-specific targeting: A recent overview. Eur. J. Med. Chem., 139 (2017) 542-563.

[5] S. Patterson, S. Wyllie, Nitro drugs for the treatment of trypanosomat id diseases: past, present, and future prospects, Trends Parasitol. 30 (2014) 289-298.

[6] W.A. Denny, Prodrugs for Gene-Directed Enzyme-Prodrug Therapy (Suicide Gene Therapy). J. Biomed. Biotechnol. 1 (2003) 48-70.

[7] R.J. Knox, M.P. Boland, F. Friedlos, B. Coles, C. Southan, J.J. Roberts, The nitroreductase enzyme in Walker cells that activates 5-(aziridin-1-yl)-2,4-dinitrobenzamide

(CB 1954) to 5(aziridin-1-yl)-4-hydroxylamino-2-nitrobenzamide is a form of NAD(P)H dehydrogenase (quinone) (EC 1.6.99.2). Biochem. Pharmacol. 37 (1988) 4671-4677.

[8] J.A. Bridgewater, R.J. Knox, J.D. Pitts, M.K. Collins, C.J. Springer, The bystander effect of the nitroreductase/CB 1954 enzyme/prodrug system is due to a cell-permeable metabolite. Hum. Gene Ther. 8 (1997) 709-717.

[9] J.V.E. Chan-Hyams, J.N. Copp, J.B. Smaill, A.V. Patterson, D.F. Ackerley, Evaluating the abilities of diverse nitroaromatic prodrug metabolites to exit a model Gram negative vector for bacterial-directed enzyme-prodrug therapy. Biochem. Pharmacol. 158 (2018) 192-200.

[10] N.A. Helsby, S.J. Wheeler, F.B. Pruijn, B.D. Palmer, S. Yang, W.A. Denny, W.R. Wilson, Effect of nitroreduction on the alkylating reactivity and cytotoxicity of the 2,4-dinitrobenzamide5-aziridine CB1954 and the corresponding nitrogen mustard SN 23862: Distinct mechanisms of bioreductive activation. Chem. Res. Toxicol. 16, (2003) 469-478.

[11] N.A. Helsby, D.M. Ferry, A.V. Patterson, S.M. Pullen, W.R. Wilson, 2-Amino metabolites are key mediators of CB 1954 and SN 23862 bystander effects in nitroreductase GDEPT. Br. J. Cancer, 90 (2004) 1084-1092.

[12] A. Chandor, S. Dijols, B. Ramassamy, Y. Frapart, D. Mansuy, D. Stuehr, N. Helsby, J.L. Boucher, Metabolic activation of the antitumor drug 5-(aziridin-1-yl)-2,4-dinitrobenzamide (CB1954) by NO synthases, Chem. Res. Toxicol. 21 (2008) 836-843.

[13] P.R. Race, A.L. Lovering, S.A. White, J.I. Grove, P.F. Searle, C.W. Wrighton, E.I. Hyde, Kinetic and structural characterisation of *Escherichia coli* nitroreductase mutants showing improved efficacy for the prodrug substrate CB1954, J. Mol. Biol. 368, (2007) 481-492.

[14] W.H. Talib, M.M. Abukhader, Combinatorial Effects of Thymoquinone on the Anticancer Activity and Hepatotoxicity of the Prodrug CB1954, Sci. Pharm. 81 (2013) 519-30.

[15] E.M. Williams, R.F. Little, A.M. Mowday, M.H. Rich, J.V.E. Chan-Hyams, J.N. Copp, J.B. Smaill, A.V. Patterson, D.F. Ackerley, Nitroreductase gene-directed enzyme prodrug therapy: insights and advances toward clinical utility, Biochem. J., 47 (2015) 131-153.

[16] G.M. Anlezark, T. Vaughan, E. Fashola-Stone, N.P. Michael, H. Murdoch, M.A. Sims, S. Stubbs, S. Wigley, N.P. Minton, Bacillus amyloliquefaciens orthologue of *Bacillus subtilis* ywrO encodes a nitroreductase enzyme which activates the prodrug CB1954, Microbiology, 148 (2002) 297–306.

[17] G.A. Prosser, J.N. Copp, S.P. Syddall, E.M. Williams, J.B. Smaill, W.R. Wilson, A.V. Patterson, D.F. Ackerley, Discovery and evaluation of Escherichia coli nitroreductases that activate the anti-cancer prodrug CB1954, Biochemical Pharmacology, 79 (2010) 678-87.

[18] A. Çelik, G. Yetiş, An unusually cold active nitroreductase for prodrug activations. Bioorg. Med. Chem. 20 (2012) 3540-3550.

[19] G.A. Prosser, J.N. Copp, A.M. Mowday, C.P. Guise, S.P. Syddall, E.M. Williams, C.N. Horvat, P.M. Swe, A. Ashoorzadeh, W.A. Denny, J.B. Smaill, A.V. Patterson, D.F. Ackerley Creation and screening of a multi-family bacterial oxidoreductase library to discover novel nitroreductases that efficiently activate the bioreductive prodrugs CB1954 and PR-104A. Biochem. Pharmacol. 85 (2013) 1091-103.

[20] K.J. Robins, D.O. Hooks, B.H.A. Rehm, D.F. Ackerley, Escherichia coli NemA is an efficient chromate reductase that can be biologically immobilized to provide a cell free system for remediation of hexavalent chromium, PLoS One 8 (2013) e59200.

[21] K.L. Green, A.M. Storey, M.E. Williams, V.A. Patterson, B.J. Smaill, N.J. Copp, F.D. Ackerley, The flavin reductase MsuE Is a novel nitroreductase that can efficiently activate two promising next-generation prodrugs for genedirected enzyme prodrug therapy, Cancers, 5 (2013) 985-977.

[22] J.T. Heap, J. Theys, M. Ehsaan, A.M. Kubiak, L. Dubois, K. Paesmans, L.V. Mellaert, R. Knox, S.A. Kuehne, P. Lambin, N.P. Minton, Spores of Clostridium engineered for clinical efficacy and safety cause regression and cure of tumors in vivo, Oncotarget 5 (2014) 1761–1769.

[23] J.N. Copp, A.M. Mowday, E.M. Williams, C.P. Guise, A. Ashoorzadeh, A.V. Sharrock, J.U. Flanagan, J.B. Smaill, A.V. Patterson, D.F. Ackerley, Engineering a Multifunctional Nitroreductase for Improved Activation of Prodrugs and PET Probes for Cancer Gene Therapy. Cell Chem. Biol., 24 (2017) 391 – 403.

[24] G.M. Anlezark, R.G. Melton, R.F. Sherwood, W.R. Wilson, W.A. Denny, B.D. Palmer, R.J. Knox, F. Friedlos, A. Williams Bioactivation of dinitrobenzamide mustards by an E. Coli B nitroreductase. Biochem. Pharmacol., 50 (1995) 609-618.

[25] P.F. Searle, M.J. Chen, L. Hu, P.R. Race, A.L. Lovering, J.I., Grove, C. Guise, M. Jaberipour, N.D. James, V. Mautner, L.S. Young, D.J. Kerr, A. Mountain, S.A. White, E.I. Hyde, Nitroreductase: A prodrug-activating enzyme for cancer gene therapy. Clin. Exp. Pharmacol. Physiol., 31 (2004) 811-816.

[26] A.V. Patterson, D.M. Ferry, S.J. Edmunds, Y. Gu, R.S. Singleton, K. Patel, S.M. Pullen, K.O. Hicks, S.P. Syddall, G.J. Atwell, S. Yang, W.A. Denny, W.R. Wilson, Mechanism of action and preclinical antitumor activity of the novel hypoxia-activated DNA cross-linking agent PR-104. Clin. Cancer Res. 13 (2007) 3922-3932.

[27] Y. Gu, A.V. Patterson, G.J. Atwell, S.B. Chernikova, J.M. Brown, L.H. Thompson, W.R. Wilson, Roles of DNA repair and reductase activity in the cytotoxicity of the hypoxia-activated dinitrobenzamide mustard PR-104A, Mol. Cancer Ther. 8 (2009) 1714-1723.

[28] M.J. McKeage, Y. Gu, W.R. Wilson, A. Hill, K. Amies, T.J. Melink, M.B. Jameson,. A phase I trial of PR-104, a pre-prodrug of the bioreductive prodrug PR-104A, given weekly to solid tumour patients, BMC Cancer 11 (2011) 432.

[29] M.R. Abbattista, S.M.F. Jamieson, Y. Gu, J.E. Nickel, S.M. Pullen, A.V. Patterson, W.R. Wilson, C.P. Guise, Pre-clinical activity of PR-104 as monotherapy and in combination with sorafenib in hepatocellular carcinoma, Cancer Biol. Ther. 16 (2015) 610–622.

[30] A.M. Mowday, A. Ashoorzadeh, E.M. Williams, J.N. Copp, S. Silva, M.R. Bull, M.R. Abbattista, R.F. Anderson, J.U. Flanagan, C.P. Guise, D.F. Ackerley, J.B. Smaill, A.V. Patterson Rational design of an AKR1C3-resistant analog of PR-104 for enzyme-prodrug therapy. Biochem. Pharmacol. 116 (2016) 176-87.

[31] Q. Jiang, Z. Zhang, J. Lu, Y. Huang, Z. Lu, Y. Tan, Q. Jiang, A novel nitro-substituted benzothiadiazole as fluorescent probe for tumor cells under hypoxic condition. Bioorgan. Med. Chem., 21 (2013) 7735-7741.

[32] Y. Zhou; Bobba, K. N.; Lv, X. W.; Yang, D.; Velusamy, N.; Zhang, J. F.; Bhuniya, S. A biotinylated piperazine-rhodol derivative: a 'turn-on' probe for nitroreductase triggered hypoxia imaging, Analyst, 2017, 142, 345–350.

[33] X. Ao, S.A. Bright, N.C. Taylor, R.B.P. Elmes, 2-Nitroimidazole based fluorescent probes for nitroreductase; monitoring reductive stress in cellulo, Org. Biomol. Chem. 15 (2017) 6104-6108.

[34] X. Zhang, Q. Zhao, Y. Li, X. Duan, Y. Tang, Multifunctional Probe Based on Cationic Conjugated Polymers for Nitroreductase-Related Analysis: Sensing, Hypoxia Diagnosis, and Imaging. Anal. Chem. 89 (2017) 5503−5510.

[35] R. Fukai, X. Zheng, K. Motoshima, A. Tai, F. Yazama, H. Kakuta, Design and Synthesis of Novel Cyclooxygenase-1 Inhibitors as Analgesics: 5-Amino-2-ethoxy-N-(substitutedphenyl) Benzamides, ChemMedChem, 6 (2011) 550 – 560.

[36] M. Xin, L. Zhang, J. Wen, H. Shen, X. Zhao, Q. Jin, F. Tang, Introduction of fluorine to phenyl group of 4-(2-pyrimidinylamino)benzamides leading to a series of potent hedgehog signaling pathway inhibitors. Bioorg. Med. Chem. Lett. 27 (2017) 3259-3263.

1113 [37] X. Li, Y. Zhang, Y. Jiang, J. Wu, E.S. Inks, C.J. Chou, S. Gao, J. Hou, Q. Ding, J. Li, X.
1114 Wang, Y. Huang, W. Xu, Selective HDAC inhibitors with potent oral activity against
1115 leukemia and colorectal cancer: Design, structure-activity relationship and antitumor activity
1116 study, Eur. J. Med. Chem. 134 (2017) 185-206.
1117 [38] T.B. Tümer, F.C. Önder, H. İpek, T. Güngör, S. Savranoğlu, T.T. Tok, A. Çelik, M. Ay,
1118 Biological evaluation and molecular docking studies of nitro benzamide derivatives with
1119 respect to *in vitro* antiinflammatory activity. International Immunopharmacol. 43 (2017) 129–
1120 139.
1121 [39] T. Güngör, G.A. Yetiş, F.C. Önder, E. Tokay, T.T. Tok, A. Celik, M. Ay, F. Köçkar
1122 Prodrugs for Nitroreductase Based Cancer Therapy-1: Metabolite Profile, Cell Cytotoxicity
1123 and Molecular Modeling Interactions of Nitro Benzamides with Ssap-NtrB, Medicinal
1124 Chemistry, 14 (2018) 495-507.
1125 [40] P. Hrobárik, I. Sigmundová, P. Zahradník, P. Kasák, V. Arion, E. Franz, K. Clays,
1126 Molecular Engineering of Benzothiazolium Salts with Large Quadratic Hyperpolarizabilities:
1127 Can Auxiliary Electron-Withdrawing Groups Enhance Nonlinear Optical Responses? J. Phys.
1128 Chem. C, 114 (2010) 22289-22302.
1129 [41] C.A. Lipinski, F. Lombardo, B.W. Dominy, Experimental and computational approaches
1130 to estimate solubility and permeability in drug discovery and development settings. Adv.
1131 Drug Deliv. Rev. 46 (2001) 3-26.
1132 [42] D.F. Veber, S.R. Johnson, H.Y. Cheng, B.R. Smith, K.W. Ward, K.D. Kopple,
1133 Molecular properties that influence the oral bioavailability of drug candidates, J. Med. Chem.
1134 45 (2002) 2615-2623.
1135 [43] Dassault Systemes Biovia, Discovery Studio Modeling Environment Release 2017,
1136 Dassault Systemes, San Diego, 2016.

[44] W.J. Egan, G. Lauri, Prediction of intestinal permeability, Adv. Drug Del. Rev. 54 (2002) 273-289.

[45] W.J. Egan, K.M. Merz, J.J. Baldwin, Prediction of Drug Absorption Using Multivariate Statistics. J. Med. Chem. 43 (2000) 3867-3877.

[46] R.J. Hron, B.C. Jursic, D.M. Neumann, Synthesis of N-aryl and N-arylcarbamoylaminoderivatives of 1,3-diazinane-5-carboxamide and their activity against glioblastoma LN-229 cell line. Bioorg. Med. Chem. 24 (2016) 6183-6193.

[47] E.H. Kerns, L. Di, Drug-Like Properties: Concepts, Structure Design and Methods: From ADME to ToxicityOptimization, Academic Press: London, Elsevier, UK, (2008) 43-47.

[48] B. Liang, H.Y. Cheng, D.Y. Kong, S.H. Gao, F. Sun, D. Cui, F.Y. Kong, Zhou, W.Z. Liu, N.Q. Ren, W.M. Wu, A.J. Wang, D.J. Lee, Accelerated Reduction of Chlorinated Nitroaromatic Antibiotic Chloramphenicol by Biocathode, Environ. Sci. Technol. 47 (2013) 5353–5361.

[49] E. Tokay, F. Kockar, Identification of intracellular pathways through which TGF-β1 upregulates URG-4/URGCP gene expression in hepatoma cells, Life Sci, 144 (2016) 121-128.

[50] M. Bös, A.J. Seleight, T. Godel, J.R. Martin, C. Riemer, H. Stadler, 5-HT6 receptor antagonists: lead optimisation and biological evaluation of N-aryl and N-heteroaryl 4-amino-benzene sulfonamides. Eur. J. Med. Chem. 36 (2001) 165-178.

[51] J.J, Blanksma, Derivatives of 3,5-dinitroaniline. Recl. Trav. Ch. Pays-Ba, 53 (1934) 988-1000.

[52] B.W. Sharp, D. Warburton, R.B. Williams, K.R.H. Wooldridge, Anticoccidial N-acyl-3,5-dinitroanilines, Ger. Offen. DE 2414084 (1974) A1 19741003.

[53] B. Kiumar, M.M. Khodaei, M. Tajik, Trimethylsilyl chloride-promoted selective desulfurization of thiocarbonyls to carbonyls with hydrogen peroxide. Synthesis, 24 (2010) 4282-4286.

1162 [54] J.A. Ratcliffe, R.J.A. Walsh, T.N. Majid, S. Thurairatnam, S. Amendola, D.J. Aldous,
1163 E.J. Souness, C. Nemecek, S. Wentzler, C. Venot, Indolizines as kinase protein inhibitors.
1164 PCT Int. Appl., (2003) 2003024967.
1165 [55] T.G. George, J. Johnsamuel, D.A. Delfín, A. Yakovich, M. Mukherjee, M.A. Phelps, J.T.
1166 Dalton, D.L. Sackett, M. Kaiser, R. Brun, K.A. Werbovetz, Antikinetoplastid antimitotic
1167 activity and metabolic stability of dinitroaniline sulfonamides and benzamides. Bioorgan.
1168 Med. Chem. 14 (2006) 5699-5710.
1169 [56] W.B. Van Horssen, Nitration of benzanilide and its derivatives. Recl. Trav. Ch. Pays-Ba,
1170 55 (1936) 245-62.
1171 [57] S. Grudzinski, M. Misiak, Studies on cyanomethyl esters. II. Reactions of cyanomethyl
1172 esters of carboxylic acids with ethylenediamine. L. Towarz. N. Wydzial III, Acta Chim. 8
1173 (1962) 119-130.
1174 [58] T. Hishiya, H. Asanuma, M. Komiyama, Molecularly Imprinted Cyclodextrin Polymers
1175 as Stationary Phases of High Performance Liquid Chromatography. Polym. J. 35 (2003) 440-
1176 445.
1177 [59] C. Siebenmann, R.J. Schnitzer, Chemotherapeutic study of p-nitrobenzoyl and related
1178 compounds. J. Am. Chem. Soc., 65 (1943) 2126-2128.
1179 [60] S.P. Anthony, M.J. Prakash, T.P. Radhakrishnan, C2-Symmetric Bis(amide) Molecules:
1180 Solid-State Assembly, Thermal Stability, and Second Harmonic Generation, Mol. Cryst. Liq.
1181 Cryst. 473 (2007) 67-85.
1182 [61] S.P. Anthony, K. Basavaiah, T.P. Radhakrishnan, Chiral Vicinal Bis(Amide) Molecules:
1183 Polar/Helical Assemblies In Crystals And Second Harmonic Generation, Cryst. Growth Des.
1184 5 (2005) 1663-1666.
1185 [62] F.R. Hewgill, P.R. Jefferıes, The Epimeric (±)-1:3-Diaminocyclohexanes. Journal of the
1186 Chemical Society, (1956) 805-808.

[63] L. Keurulainen, O. Salin, A. Siiskonen, J.M. Kern, J. Alvesalo, P. Kiuru, M. Maass, J.Y. Kauhaluoma, P. Vuorela, Design and Synthesis of 2-Arylbenzimidazoles and Evaluation of Their Inhibitory Effect against Chlamydia pneumoniae. J. Med. Chem., 53 (2010) 7664-7674.

[64] P.G. Nair, C.P. Joshua, Mixed benzoic N-alkyldithiocarbamic anhydride. Convenient reagent for benzoylation. Indian Journal of Chemistry, 13 (1975) 35-37.

[65] E.K. Rao, V. Sasisekharan, Synthesis of distamycin and netropsin analogs. Part II. DNA binding bisquaternary ammonium heterocycles analogs to NSC 101327. Indian Journal of Chemistry, Section B: Organic Chemistry Including Medicinal Chemistry, 29B (1990) 503-507.

[66] Gaussian 09, Revision E.01, M.J. Frisch, G.W. Trucks, H.B. Schlegel, G.E. Scuseria, M.A. Robb, J.R. Cheeseman, G. Scalmani, V. Barone, B. Mennucci, G.A. Petersson, Gaussian, Inc., Wallingford, CT, USA, 2009.

[67] B.R. Brooks, R.E. Bruccoleri, B.D. Olafson, D.J. States, S. Swaminathan, M. Karplus, CHARMM: A program for macromolecular energy minimization and dynamics calculations, J. Comput. Chem. 4 (1983) 187–217.

[68] P. Houghton, R. Fang, I. Techatanawat, G. Steventon, P.J. Hylands, C.C. Lee, The sulphorhodamine (SRB) assay and other approaches to testing plant extracts and derived compounds for activities related to reputed anticancer activity, Science Direct Methods, 42 (2007) 377–387.

1212 **GRAPHICAL ABSTRACT**

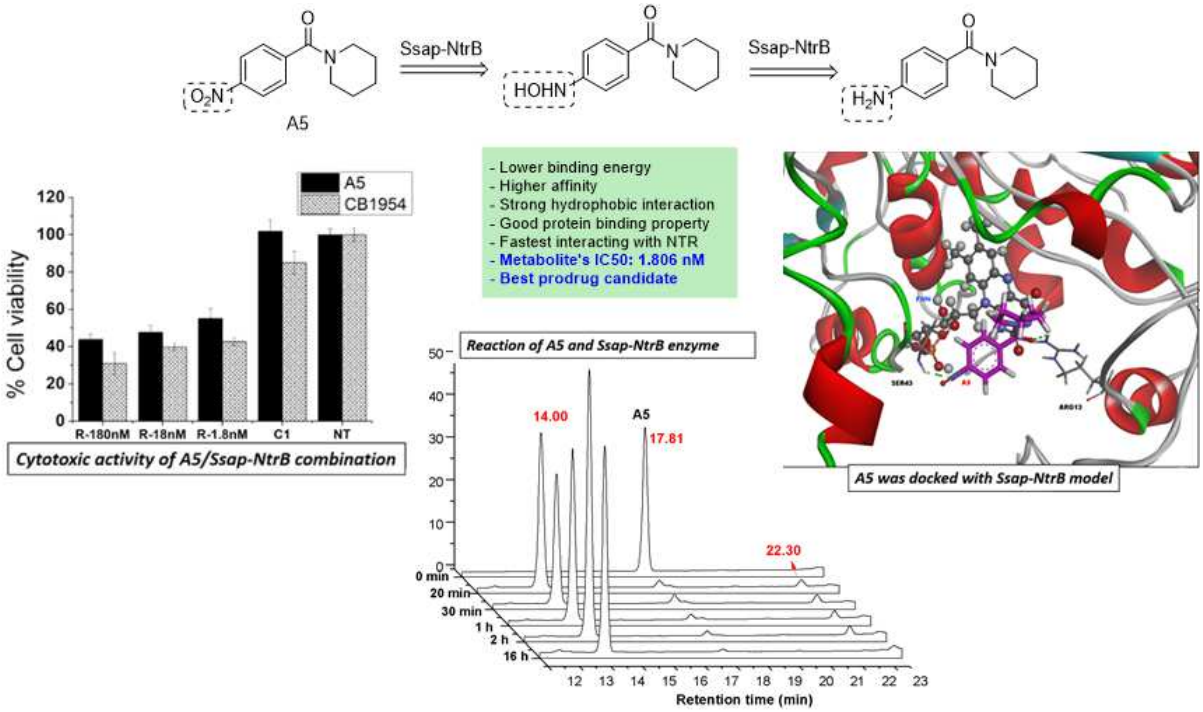

1213

1214

1215

1216

PRODRUGS FOR NITROREDUCTASE BASED CANCER THERAPY- 2

Novel Amide/Ntr Combinations Targeting PC3 Cancer Cells

Tuğba Güngör[a], Ferah Cömert Önder[a], Esra Tokay[b], Ünzile Güven Gülhan[c], Nelin Hacıoğlu[b], Tuğba Taşkın Tok[d], Ayhan Çelik[c, #] Feray Köçkar[b], Mehmet Ay[a*]

[a]Department of Chemistry, Faculty of Sciences and Arts, Natural Products and Drug Research Laboratory, Çanakkale Onsekiz Mart University, Çanakkale 17020, Turkey

[b]Department of Molecular Biology and Genetic, Faculty of Sciences and Arts, Balıkesir University, Balıkesir 10145, Turkey

[c]Department of Chemistry, Faculty of Science, Gebze Technical University, Gebze-Kocaeli 41400, Turkey

[d]Department of Chemistry, Faculty of Sciences and Arts, Gaziantep University, Gaziantep 27310, Turkey

Highlights

- Nitro containing aromatic amide prodrugs **(A1-A23)** were designed and synthesized.
- Enzymatic interactions of prodrug candidates with a novel nitroreductase enzyme, Ssap-NtrB were investigated.
- Prodrug candidates and their metabolites were tested against different cancer cells.
- Enzyme-prodrug interactions by in silico ADMET and molecular docking techniques were analyzed.
- Some prodrugs were found toxic against PC3 cell (IC_{50} values of some metabolites were determined at nM level)
- In a result of theoretical and biological studies, combinations of **A5, A6** and **A20** with Ssap-NtrB can be suggested as potential prodrugs/enzyme combinations to be used for NTR based cancer therapy compared with CB1954/NfsB.